



**DESIGN AND GROUND-TESTING OF AN INFLATABLE-RIGIDIZABLE
STRUCTURE EXPERIMENT IN PREPARATION FOR SPACE FLIGHT**

THESIS

Chad R. Moeller, Capt, USAF

AFIT/GA/ENY/05-J02

**DEPARTMENT OF THE AIR FORCE
AIR UNIVERSITY**

AIR FORCE INSTITUTE OF TECHNOLOGY

Wright-Patterson Air Force Base, Ohio

APPROVED FOR PUBLIC RELEASE; DISTRIBUTION UNLIMITED

The views expressed in this thesis are those of the author and do not reflect the official policy or position of the United States Air Force, Department of Defense, or the U.S. Government.

AFIT/GA/ENY/05-J02

**DESIGN AND GROUND-TESTING OF AN INFLATABLE-RIGIDIZABLE
STRUCTURE EXPERIMENT IN PREPARATION FOR SPACE FLIGHT**

THESIS

Presented to the Faculty

Department of Aeronautics and Astronautics

Graduate School of Engineering and Management

Air Force Institute of Technology

Air University

Air Education and Training Command

In Partial Fulfillment of the Requirements for the
Degree of Master of Science in Astronautical Engineering

Chad R. Moeller, BS

Capt, USAF

June 2005

APPROVED FOR PUBLIC RELEASE; DISTRIBUTION UNLIMITED

**DESIGN AND GROUND-TESTING OF AN INFLATABLE-RIGIDIZABLE
STRUCTURE EXPERIMENT IN PREPARATION FOR SPACE FLIGHT**

Chad R. Moeller, BS

Capt, USAF

Approved:

_____/signed/_____
Richard G. Cobb, PhD (Chairman)

Date

_____/signed/_____
Anthony N. Palazotto, PhD (Member)

Date

_____/signed/_____
Nathan A. Titus, PhD (Member)

Date

AFIT/GA/ENY/05-J02

To My Wife

Acknowledgments

I would like to thank God and my family and friends for supporting me throughout this entire endeavor. Above all I want to thank my wife; I couldn't have done it without her constant love and support.

I'd like to also thank my advisor, Dr. Rich Cobb for providing insight and innovation in solving the many complex problems presented by RIGEX, and for his experience and guidance through the mires of information RIGEX has to offer.

I especially want to thank my lab technician, Mr. Wilbur Lacy, who went above and beyond with his constant solutions to my last minute emergencies.

Chad R. Moeller

Table of Contents

	Page
Acknowledgments.....	v
Table of Contents.....	vii
List of Figures.....	ix
Abstract.....	2
I. Introduction.....	3
<i>Background</i>	3
<i>Problem Statement</i>	4
<i>RIGEX Background</i>	7
<i>Research Objectives</i>	11
<i>Assumptions/Constraints</i>	11
<i>Thesis Summary</i>	12
II. Literature Review.....	13
<i>Chapter Overview</i>	13
<i>History of Inflatables and Inflatable-Rigidizables</i>	13
<i>Current Inflatable/Rigidizable Research</i>	14
<i>Sub-Tg Rigidization</i>	14
<i>Other Methods of Rigidization</i>	17
<i>Other Current Projects</i>	19
<i>Space Experiment Review Board (SERB) / Space Test Program (STP)</i>	22
<i>Payload Envelope</i>	24
<i>RIGEX Power Supply</i>	26
<i>Current Status of RIGEX</i>	27
<i>Chapter Summary</i>	28
III. Methodology.....	29
<i>Chapter Overview</i>	29
<i>Experiment Assembly</i>	29
<i>Inflation Tests</i>	30
<i>Pressure Vessel Volume Determination</i>	33
<i>Inflation Test Setup and Procedures</i>	39

	Page
<i>Thermal Tests</i>	42
<i>Cooling Profile Determination</i>	48
<i>Thermal Test Setup and Procedures</i>	57
<i>Chapter Summary</i>	60
IV. Analysis and Results	61
<i>Chapter Overview</i>	61
<i>Inflation Tests</i>	61
<i>Thermal Tests</i>	66
<i>Overall Analysis and Results</i>	72
<i>Chapter Summary</i>	73
V. Conclusions and Recommendations	74
<i>Chapter Overview</i>	74
<i>Conclusions</i>	74
<i>Recommendations</i>	77
<i>Summary</i>	80
Appendix A. Mathcad [®] Pressure Vessel Calculation Worksheet	82
Appendix B. LabVIEW Program and Test Equipment Overview	86
Appendix C. 2004 DoD SERB Briefing	89
Bibliography	99
Vita	102

List of Figures

Figure	Page
1. Inflatable Antenna Experiment (30)	4
2. Sub-Tg Tube Before and After Inflation and Rigidization.....	7
3. RIGEX Preliminary Design (3)	9
4. Heater Box Evolution	10
5. NASA Echo I Passive Communication Satellite (6).....	13
6. SSP Being Lifted by Two Fingers	15
7. STR Aluminum Laminate Boom.....	18
8. Inflatable/Self-Rigidizable Reflectarray Antenna.....	18
9. Deployable Structures Experiment	20
10. ISAT's Deployment Demonstration of a Large Space Structure (32).....	20
11. SBR Coverage in MEO vs. LEO (32).....	21
12. The SERB Process (27)	23
13. STP Mission Life Cycle Activities	24
14. GAS Container.....	25
15. CAPE Canister	25
16. One of Eight Battery Packs Used to Power RIGEX.....	26
17. Quarter Structure and Vacuum Chamber.....	30
18. Battery Storage Volume.....	32
19. Pressure System Layout.....	34
20. Pressure System Breakdown.....	35

Figure	Page
21. Size Comparison of 50cm ³ vs. 500cm ³ Vessel	38
22. Redesigned Pressure System.....	39
23. Cloth and Sub-Tg Tubes	40
24. Solenoid Operation	40
25. Heater Box Composition.....	42
26. Minco Thermofoil TM Resistive Heaters	43
27. Resistive Heater Wiring Diagrams (21).....	44
28. Thermocouple Locations for Heating Differential Test (14).....	45
29. Heating Differential Across the Tube (14)	46
30. Cooling Profile Thermocouple Locations.....	47
31. Major Surfaces Involved in Radiation Analysis	49
32. Calculated Sub-Tg Tube Cooling Profile, -60°C Ambient Temperature	54
33. Calculated Sub-Tg Tube Cooling Profile, -40°C Ambient Temperature	54
34. Calculated Sub-Tg Tube Cooling Profile, 30°C Ambient Temperature.....	55
35. Calculated Sub-Tg Tube Cooling Profile, 55°C Ambient Temperature.....	55
36. Calculated Sub-Tg Tube Cooling Profile, 85°C Ambient Temperature.....	56
37. Example Spreadsheet Used for Tracking Tests	59
38. Plastic Tubing Connection.....	62
39. Sub-Tg Tube Pressurization.....	63
40. Cloth Tube Pressurization.....	64
41. Tubes not Fully Inflated.....	65

Figure	Page
42. Sub-Tg Tube Thermal Profile.....	67
43. Sub-Tg Tube Cooling Profile.....	68
44. Experimental vs. Analytical Cooling Profile – Hot Thermocouple.....	69
45. Experimental vs. Analytical Cooling Profile – Cool Thermocouple.....	70
46. Sub-Tg Pressure and Thermal Profile during Deployment.....	72
47. Initial Pressure System Concept (3).....	74
48. First Assembly of Pressure System (21).....	75
49. Second Assembly of Pressure System (14.....	75
50. Final Design of Pressure System	76
51. NI Modules/Docking Station	86
52. Endevco Pressure Meters.....	86
53. Agilent System Power Supply	87
54. Hewlett-Packard Dual DC Power Supplies	88

List of Tables

Table	Page
1. RIGEX Concept of Operations (14)	5
2. RIGEX Modification History	10
3. Advantages and Disadvantages of Sub-Tg Rigidization	16
4. Comparison of Payload Envelopes	25
5. Status of RIGEX before Current Thesis Work	28
6. Total System Pressures and Vessel Dimensions.....	37
7. Original vs. Modified Pressurization System	38
8. Minco Thermofoil TM Heater Resistances.....	44
9. Sub-Tg Tube Constants.....	52
10. Time to Event Temperatures.....	56
11. Analytic vs. Experimental Pressurization Results	62
12. Tube Heating Times.....	67
13. Predicted vs. Experimental Key Events.....	71
14. Status of RIGEX after Current Thesis Work	81

Abstract

As the demand for larger space structures increases, complications arise including physical dimensions, weight, and launch costs. These constraints have forced the space industry to look for smaller, more lightweight, and cost-effective solutions.

Future antennas, solar sails, sun shields, and other structures have the potential to be exponentially larger than their launch envelopes. Current research in this area is focused on the use of inflatable, rigidizable structures to reduce payload size and mass, ultimately reducing launch costs. These structures can be used as booms, trusses, wings, or can be configured to almost any simple shape. More complex shapes can be constructed by joining smaller rigidizable/inflatable members together. Analysis of these structures must be accomplished to validate the technology and gather risk mitigation data before they can be widely used in space applications.

The Rigidizable, Inflatable, Get-Away-Special Experiment (RIGEX) was created to test structures that meet the aforementioned demand for smaller, more lightweight, and cost effective solutions to launching payloads into space. The purpose of this experiment is to analyze the effects of the space environment on inflatable, rigidizable structural components and validate ground-test procedures for these structures.

This thesis primarily details the pressurization system enhancements and validates thermal performance for RIGEX. These enhancements and the increased knowledge of the thermal properties will improve the probability of experiment success.

DESIGN AND GROUND-TESTING OF AN INFLATABLE-RIGIDIZABLE STRUCTURE EXPERIMENT IN PREPARATION FOR SPACE FLIGHT

I. Introduction

Background

As the need for space-lift increases, so does the need for lightweight payloads that can be stowed into existing launch envelopes. Inflatable-rigidizable structures will play increasingly vital roles in all areas of future space applications due to their strong, lightweight composition and their small-payload volume. These roles include, but are not limited to, RF interferometry, SAR mapping, outer planet exploration, IR/optical interferometry, high-data rate RF communications for small spacecraft, earth radiometry and solar observations of planets (23). Also, to add to their credibility, these lightweight payloads should demonstrate deployment reliability, mechanical packaging efficiency, geometric precision, thermal stability and long-term dimensional stability (23).

Mechanical packaging efficiency is necessary to stow the largest possible structure in the smallest amount of space. For example, the 1996 Inflatable Antenna Experiment (IAE) stowed an antenna membrane reflector 50 feet (14 meter) in diameter, three 92-foot (28 meter) struts, and all support equipment into an envelope volume the size of a grand piano (Figure 1).

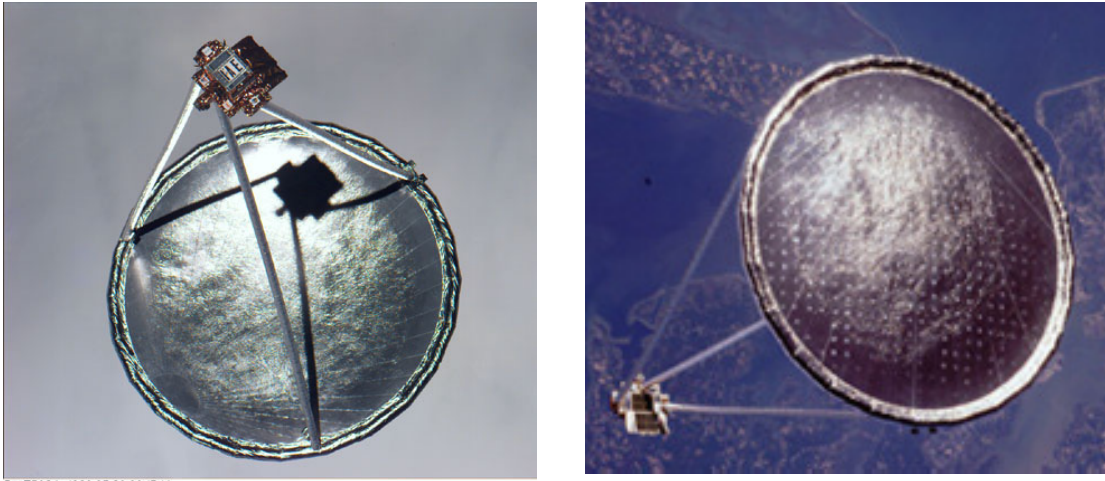


Figure 1: Inflatable Antenna Experiment (30)

Above all, payloads must demonstrate cost-effectiveness to justify their use in space. In addition to the size and weight advantages stated previously, inflatable-rigidizables hold large potential in engineering and production cost savings. The IAE flight experiment cost was on the order of \$1,000,000. This represents substantial savings over comparable mechanical systems which may cost as much as 10 to 100 times more (5, 30).

Problem Statement

As originally conceived by Captain John D. DiSebastian, the ultimate objective of the Rigidized Inflatable Get-Away-Special Experiment (RIGEX) is to “enable the application of large-scale inflated and rigidized space structures to operational space systems.” The specific objective for RIGEX is “To verify and validate ground testing of

inflation and rigidization methods for inflatable space structures against zero-gravity space environment” (3).

Both of the above statements affirm the drivers behind this endeavor. Shown below in Table 1 is the overall Concept of Operations (CONOPS) for RIGEX (14). To date, no inflatable-rigidizable structure has undergone spaceflight. As mentioned above with the IAE and again in Chapter II, the only inflatable structures which have been in space are simply that – inflatable, but not rigidizable. As such they are prone to losing pressure and therefore their usefulness over time. The tubes themselves will demonstrate the inflatable-rigidizable technology and return useful information on their structural and material properties, while the deployment process will demonstrate a valid method of deploying the tubes. Overall, RIGEX will validate this new technology.

Table 1: RIGEX Concept of Operations (14)

EVENT	DESCRIPTION
Launch	Shuttle Takeoff
Activate Environmental Heaters	TBD if available on CAPE
Computer on	Boot-up & diagnostic
Activate Environmental Sensors	After specified wait period
1st failsafe point	(in case of inadvertent restart)
Inflation process	Heat and inflate all tubes
Venting process	Vent all tubes to ensure structural stiffness
Excitation process	Vibrate tubes and observe modal response
2nd failsafe point	(in case of inadvertent restart)
Shutdown flight computer	Prepare for mission end
Turn off power to environmental Heaters	Shuttle crew preparing for reentry
Land and recovery	Collect experiment

The experiment utilizes tubes composed of thermoset plastic matrixed with graphite/epoxy and sheathed in Kapton inside and out. They have a relatively low glass-transition temperature of 125°C (which is tailorable) and will therefore be referred to as ‘sub-Tg tubes’ or simply ‘tubes’ throughout this thesis. The tubes are produced by L’Garde of Tustin, California. L’Garde was founded in 1971 to analyze, design, manufacture, test and fly inflatable space structural systems and has produced many successful inflatable experiments (13).

To expand on the CONOPS stated previously, RIGEX will heat a folded sub-Tg tube, inflate, cool to a rigid state, vibrate using piezoelectric actuators, and collect data on the deployment process and tube modal characteristics. This process will be iterated on orbit for three separate but identical tubes.

Each tube is 20 inches long, the maximum length that would fit in the original payload envelope. The tubes have five folds each. This is due to the final inflated length of the tube and to assist in heating. If the folds were any wider, the heating differential across the tube would cause problems due to some portions of the tube being much cooler than others. This will be discussed in detail in Chapter III. If the folds were any smaller, the stressed caused by the small curvature of the folds could potentially damage the material. The current form allows relatively even heating and a small enough size to be packaged easily.

Data on the tubes will be collected using digital imagery, environmental sensors, and tri-axial accelerometers. See Figure 2 for images of a sub-Tg tube before and after inflation and rigidization.

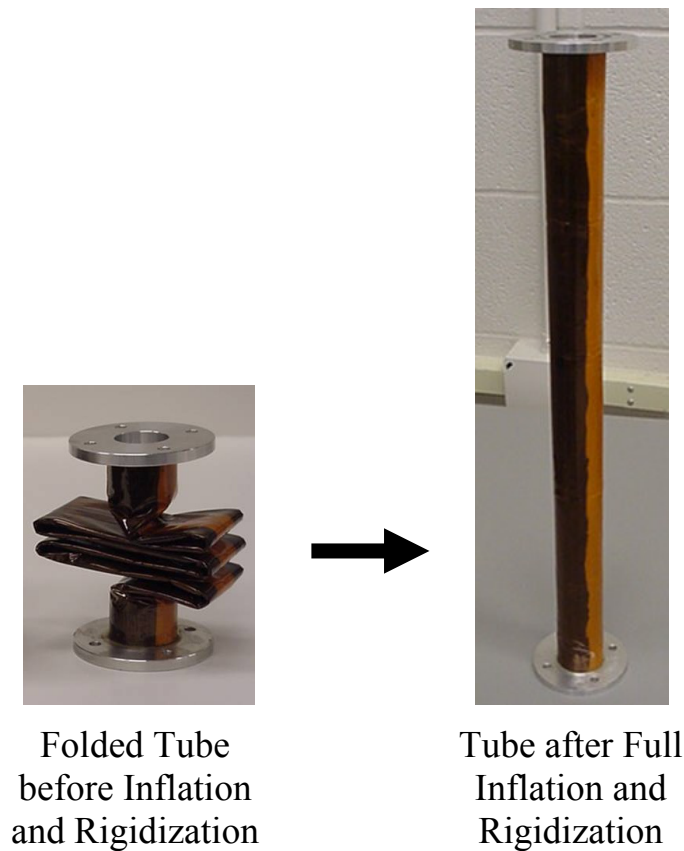


Figure 2: Sub-Tg Tube Before and After Inflation and Rigidization

RIGEX Background

RIGEX has passed through many hands on its journey towards launch and implementation. The experiment was initially researched in 2001 by Captain John D. DiSebastian III, USAF. DiSebastian conceptualized the preliminary design of RIGEX and researched in detail many of the components necessary to produce the final experiment. This study in turn, sparked the research of six subsequent theses.

Thomas G. Single (25) investigated the inflatable-rigidizable tubes specifically by exploring the variation in vibrational data for various thermal and pressure conditions.

Thomas L. Philley (21) focused on the many subsystems of RIGEX. He validated the design and function of the thermal, pressurization, and imaging systems. Philley also created a quarter-structure prototype to test the various subsystems together inside and outside a vacuum chamber. Raymond G. Holstein (9) constructed a finite element model in ABAQUS of both the RIGEX quarter and full structures “for the purpose of manufacturing and testing a flight-worthy article capable of housing the RIGEX experimental components.” Steven N. Lindemuth (14) further tested and refined the pressurization and thermal systems, and managed the Space Shuttle manifestation process. David C. Moody (18) designed and tested the PC-104 computer software and hardware, which controls all RIGEX operations from launch to landing.

Along with the above Master’s students, summer interns from various universities have made worthwhile contributions to RIGEX. Most noteworthy are Michael Maddux (16) and Kevin Ponziani (22). Maddux and Ponziani completed detailed investigations into heater box design and digital image processing, respectively.

As the experiment passed from researcher to researcher, the designs of RIGEX subsystems have evolved to their current state. All modifications had to be consistent with NASA and more specifically the payload envelope constraints, as will be discussed in detail in Chapter II.

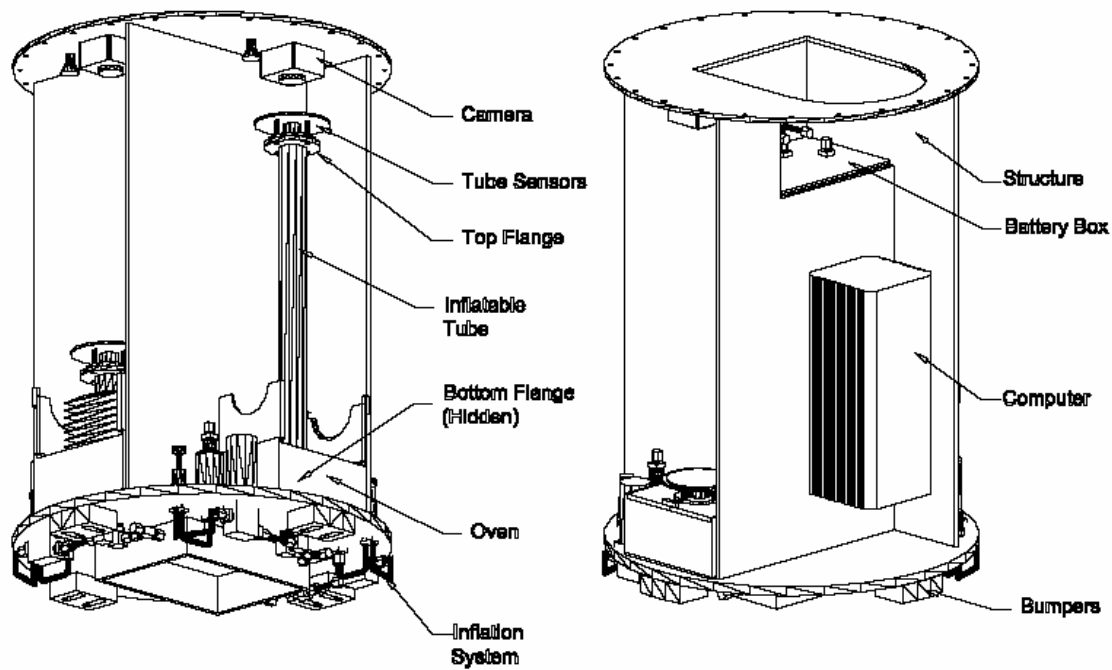


Figure 3: RIGEX Preliminary Design (3)

The preliminary design of the structure (Figure 3) has undergone only one major modification since its inception. In contrast, the pressurization system (discussed in detail in Chapter III) and heater boxes (Figure 4) have progressed through several iterations to arrive at their final design. The power system and payload envelope have evolved externally through NASA proposals and directed changes (discussed in detail in Chapter III).

In each case, the new designs evolved from initial paper concepts, problems encountered with primary functions, issues with testing or analysis results, or for opportunistic reasons. Table 2 illustrates the upgrades to each subsystem and the reasons why modifications were deemed necessary.

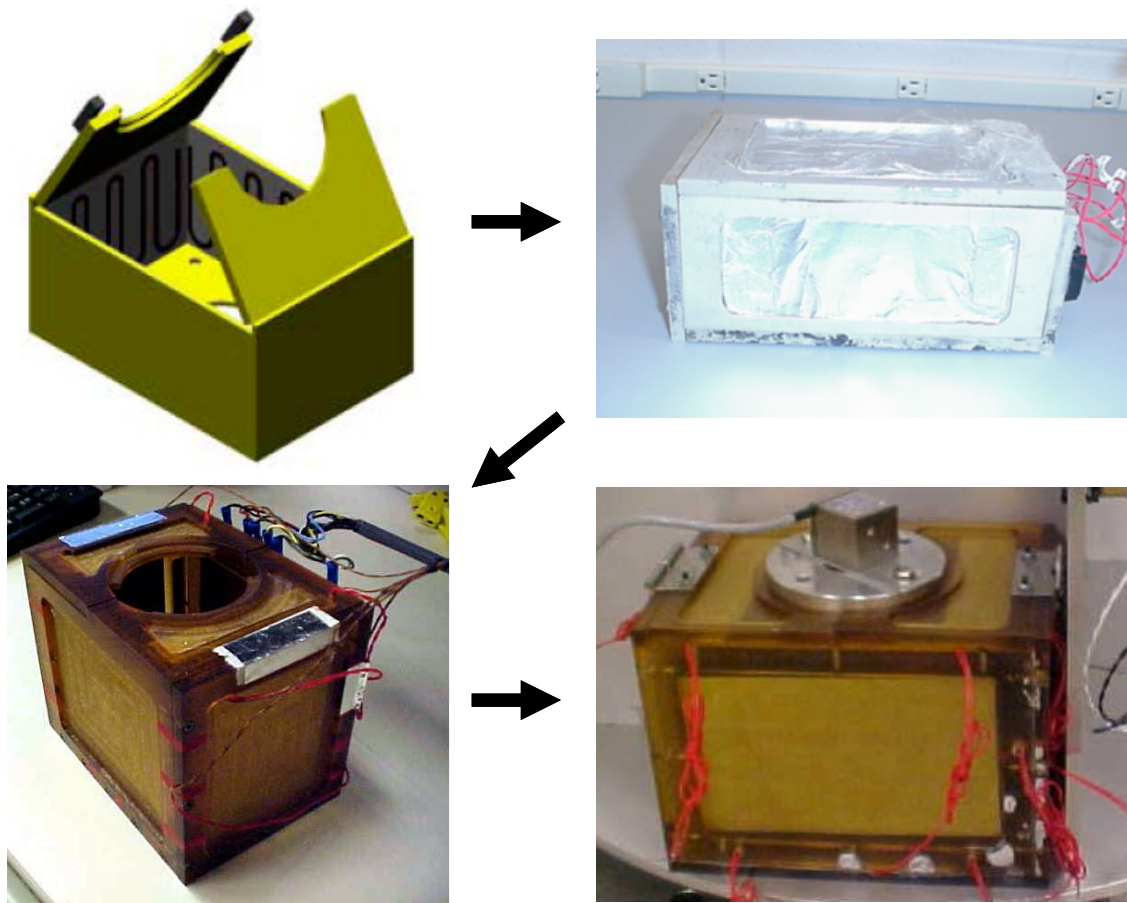


Figure 4: Heater Box Evolution

Table 2: RIGEX Modification History

Subsystem	Modification	Reason
Main Structure	Computer access port removal	Stress concentration analysis (9)
Main Structure	Component layout	Tube interference (9, 14, 18)
Heater Box	Design changes	Inadequate performance tests (16)
Heater Box	Dimensions altered	Poor fit to main structure
Pressure System	Component/layout alterations	Higher reliability and fit (14)
Pressure System	Larger pressure vessels	Higher reliability and safety
Power	Battery pack to Shuttle power	Opportunistic, envelope change

Research Objectives

The primary goals of this thesis are to improve upon the current RIGEX design by resolving critical issues encountered with the pressurization system, validate the cooling profile of the sub-Tg tubes, manage manifestation on the Space Shuttle through the Space Test Program (STP) and NASA, and incorporate any necessary changes to the experiment due to the introduction of a new payload envelope.

Assumptions/Constraints

One of the primary reasons to perform this experiment in space is the lack of a combine vacuum/zero-g environment on Earth. Zero-g simulations can only be carried out so far before the variables involved combine to produce non-realistic results. RIGEX systems are tested and simulated as closely as possible to the space environment to improve probability of success on orbit, but until the actual experiment takes place in space, the simulations and testing can not be fully validated. This experiment effort will return valuable information the deployment and characteristics of inflatable-rigidizables in space and therefore provide risk-mitigation information for future missions.

Depending on the inclination of the Shuttle cargo bay, the time RIGEX will be in and out of direct sunlight will vary. STP recommends constructing experiments for a survival temperature range of -60°C to 85°C (4). This is a relatively large range whose limits include a factor of safety. Should the temperature of the Shuttle cargo bay stay above 66°C , the piezoelectric actuators used to vibrationally excite the tubes would never be within their operating range (66°C maximum) (26). The heating and cooling profiles,

which will be fully characterized in this thesis, are a function of the shuttle bay temperature. As such, the experiment must be able to operate in a wide range of temperatures which will not be known beforehand.

NASA sets many requirements for experiments carried by the Shuttle. These include constraints on thermal, pressurization, power, center-of-gravity, structural, electromagnetic and natural frequency to name a few. AFIT must provide either analysis or test results to prove to NASA that their requirements are met. All constraints must be met or waived by NASA personnel prior to flight (4).

Thesis Summary

In subsequent chapters, investigation, testing and analysis on the goals of this thesis are presented. Chapter II discusses the history of inflatables and inflatable-rigidizables, current inflatable/rigidizable research in industry, the Space Experiment Review Board (SERB) and Space Test Program (STP), and delves into the recent changes in the RIGEX payload enclosure and power supply. Chapter III covers the methodology behind the thesis encompassing the reasoning, set-up and procedures for the testing accomplished. Chapter IV analyzes the results from the tests performed. Chapter V is comprised of the conclusions of the tests and recommendations for future research.

II. Literature Review

Chapter Overview

This chapter discusses the history of inflatables and inflatable-rigidizables, current inflatable/rigidizable research in industry, the Space Experiment Review Board (SERB) process and Space Test Program, and discusses recent changes in the RIGEX payload enclosure and power supply.

History of Inflatables and Inflatable-Rigidizables

Although inflatable space-structures have been used as far back as the NASA Echo I passive satellite system launched in 1960 (Figure 5), inflatables in space have had very limited usage since. Problems with keeping constant pressure in the systems due to micro-meteor impacts and degradation in materials from ultraviolet (UV) radiation or other sources has limited the reliability and therefore the use of inflatables in space.

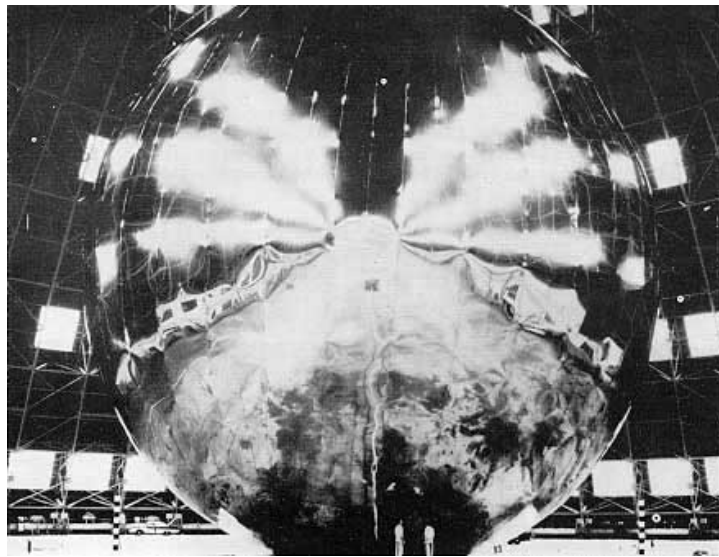


Figure 5: NASA Echo I Passive Communication Satellite (6)

ECHO I is an example of inflatable space technology in its infancy. As mentioned in Chapter I, the IAE which flew in 1996 is a more modern example of an inflatable space structure (8). It was intended to validate and characterize the mechanical function and performance of a 14-meter-diameter inflatable deployable antenna reflector structure in an operational orbit. IAE was developed by L'Garde of Tustin, CA and NASA's Jet Propulsion Laboratory (JPL) of Pasadena, CA.

During deployment, IAE's changing center-of-mass as the antenna unfurled and inflated caused pendulous and chaotic motion of the entire satellite. Also, it did not achieve the full mission objectives because it never reached its intended design pressure of 3 psi. The parabolic surface of the reflector did not become taut enough to produce the specified surface accuracy.

Even though some of IAE's mission objectives were not met, it did prove that inflatable technology can be a feasible way of stowing and deploying a large, lightweight structure into the space environment.

Current Inflatable/Rigidizable Research

Sub-Tg Rigidization

The current trend in space and space-related industry is towards inflatable structures that undergo some type of rigidization process to bring them to a structurally stiff state. This alleviates the requirement of a purely inflatable structure to retain pressure throughout its useful life. Without rigidization, inflatables are prone to pressure losses over time.

RIGEX uses the sub-Tg tubes discussed in Chapter I as a demonstration of inflatable-rigidizable technology. For RIGEX, a glass-transition (T_g) of 125°C was chosen; therefore, the tubes soften when heated above this temperature. Once they are pressurized and the material cools below the 125°C , they reach a structurally stiff state and can be vented of their pressurized gas. The T_g temperature itself can be adjusted during the manufacturing process depending on user needs.

The Space Solar Power (SSP) truss (8), also developed by L'Garde, used sub-Tg tubes ($T_g = 55^{\circ}\text{C}$) as longerons and diagonals to construct a 24-foot long truss (Figure 6). The truss only weighed 9 pounds total. SSP underwent compression tested at NASA-Langley Research Center and outperformed its predicted compression of 500 lb by 10%, failing at 556 lb.

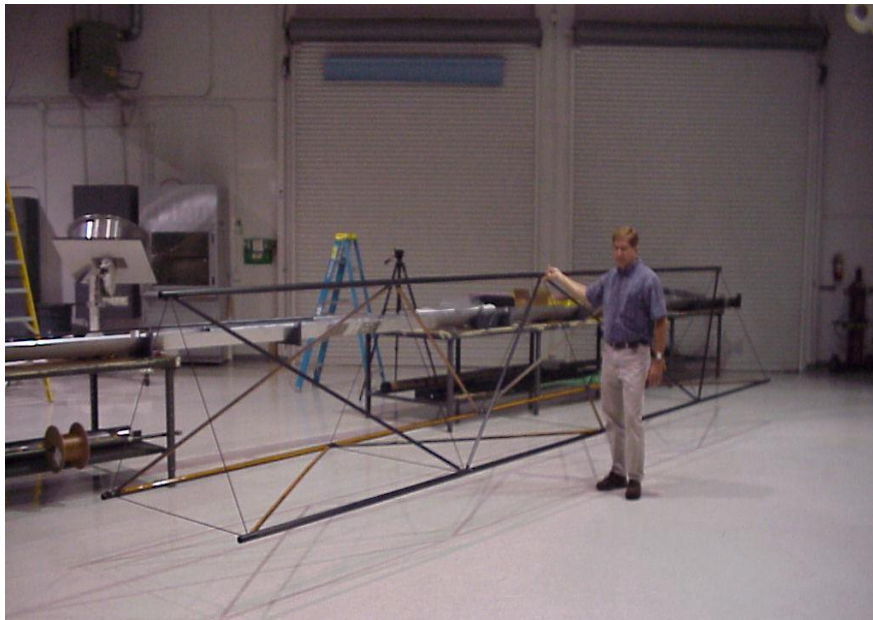


Figure 6: SSP Being Lifted by Two Fingers

According to Dr. Koorosh Guidanean, project manager for SSP, the advantages heavily outweigh the disadvantages of the sub-Tg rigidization method for space use as tested in the lab environment (Table 3) (8). The results from SSP prove the viability of the sub-Tg tubes. Between this analysis and the results to be gained in space from RIGEX, the sub-Tg method of rigidization will become a proven technology.

Table 3: Advantages and Disadvantages of Sub-Tg Rigidization (8)

Advantages	Disadvantages
Simple passive rigidization pending thermal environment	May require low power heaters pending thermal analysis
Reversible and ground testable	Thermal environment requirements
Long shelf-life	
No maximum thickness limitations	
Tailorable Tg (glass transition temperature)	
No auxiliary equipment and hardware	
Composite cured on ground under controlled condition	
Unlimited deployment life time	
Stable matrix	
No need to control pre-deployment environment	
Ability to form faultless end joints	

Other Methods of Rigidization

Heating is not the only means for an inflatable structure to rigidize. However, all methods of rigidization must involve some sort of catalyst to reach their final state. The sub-T_g tubes use temperature, but there are various other methods currently under research.

One of these methods utilizes solar UV radiation, typically between 250 and 380 nanometers, to rigidize inflatable structures. Technology under development for the “Mars Airplane” (24) uses this method. The inflatable structure is impregnated with a UV-curable resin which rigidizes when exposed to solar UV radiation (12). Using this configuration, only a UV-resistant container is needed to house the inflatable structure, therefore no heater is necessary to soften the material before deployment. One deterrent from this type of rigidization is that it is limited in structural performance because the reinforcement must be transparent to UV energy, such as with fiberglass or quartz (2). These materials do not offer the superior structural composite properties like those of graphite, which is opaque to the UV energy and therefore blocks the rigidizing material from exposure to it.

A third method of rigidization uses Spring Tape Reinforced (STR) aluminum laminate (15). The ‘spring tape’ is the same material utilized in a self-recoiling measuring tape. The STR aluminum laminate boom automatically rigidizes after it is deployed with no space power, no curing agent, and no rigidization system required. Therefore, it is called self-rigidizable technology (10). The boom is reinforced axially and circumferentially with spring tape as shown in Figure 7.

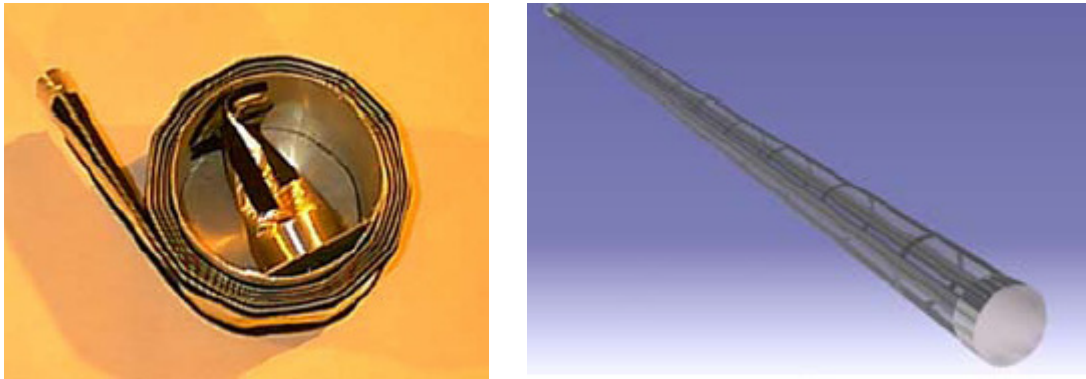


Figure 7: STR Aluminum Laminate Boom

One project utilizing STR booms is the Inflatable/Self-Rigidizable Reflectarray Antenna currently under development at JPL (Figure 8). This project uses a 3-meter reflectarray and an offset feed horn to increase aperture efficiency. Currently, a 7 to 10-meter aperture inflatable X/Ka dual-band reflectarray is being developed using the same technology. The X-band is intended for robust uplink control and command signals, while the Ka-band is for high data rate downlink transmission.

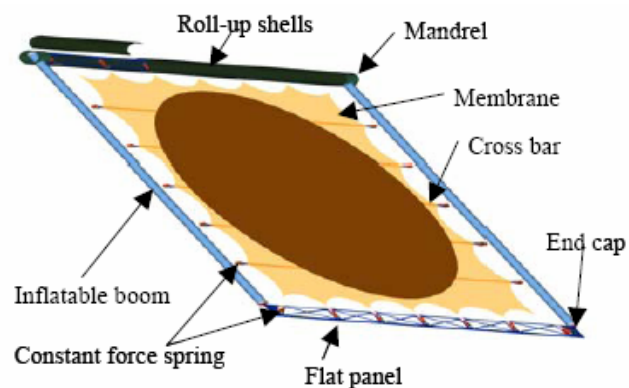
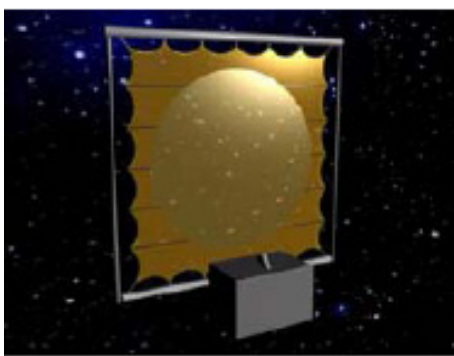


Figure 8: Inflatable/Self-Rigidizable Reflectarray Antenna (15)

Other Current Projects

The Deployable Structures Experiment (DSX), proposed by AFRL, (Figure 9) will use rigidizable materials in a 25-meter long boom and truss to analyze deployment kinematics and precision, effects of folds, joint free-play and radiation degradation of these structures in Mid-Earth Orbit (MEO) (29). The large booms and trusses are necessary to prove the feasibility for use in very large space structures. The DoD desires a validated capability to build 300-meter space structures. As an example application, a 300-meter radar in MEO can provide 24-hour tracking of individual weapons of mass destruction (29). The DSX experiment objectives are to provide remediation and survivability information in the MEO range for a wide variety of core spacecraft technologies. It is expected to have a pervasive impact across all DoD mission areas.

DSX will not be recovered, however, RIGEX will return on the Space Shuttle Orbiter. Dr. Gregory Spanjers, DSX Project Manager, has expressed interest in the results from RIGEX to analyze the fiber breakage and other properties of the deployed sub-Tg tubes (28). DSX is currently scheduled for launch after RIGEX has flown and returned. RIGEX will serve as a risk-mitigation effort for DSX and therefore future, larger DoD missions.

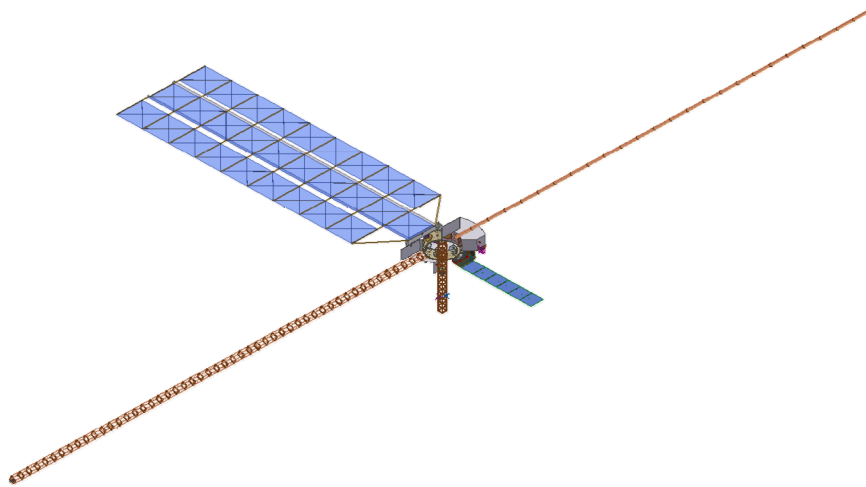


Figure 9: Deployable Structures Experiment

Another large space-structure application is the Innovative Space-Based-Radar (SBR) Antenna Technology (ISAT) experiment (32), which is currently scheduled for launch in 2009, will use a rigidizable structure on the order of 100 meters to meet its experimental objectives (Figure 10).

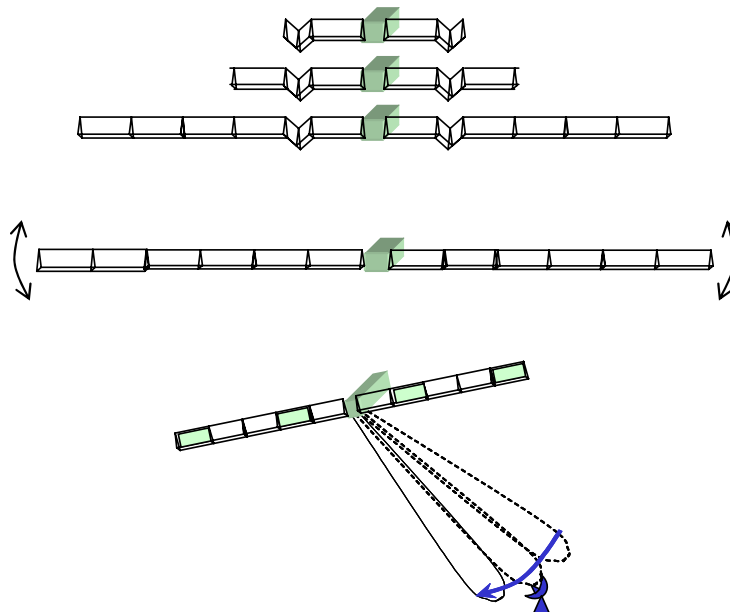


Figure 10: ISAT's Deployment Demonstration of a Large Space Structure (32)

The primary objective is to use ISAT as a test bed for demonstrating critical technologies enabling persistent, global, tactical ground movement target indicators (GMTI) and air movement target indicators (AMTI). With 300-meter aperture satellites in MEO (altitude $\approx 10,000$ km), individual targets could be tracked around the world 24-hours a day using a cluster of 12 satellites. The same mission would require 96 80 – 100-meter satellites in low-earth-orbit (LEO) to do the same job (Figure 11). Along with the reduced number of satellites, a satellite in MEO would be unaffected by a high-altitude nuclear detonation (HAND) in LEO. A detonation in LEO would disable all satellites in the same orbit within 30 – 60 days (29).

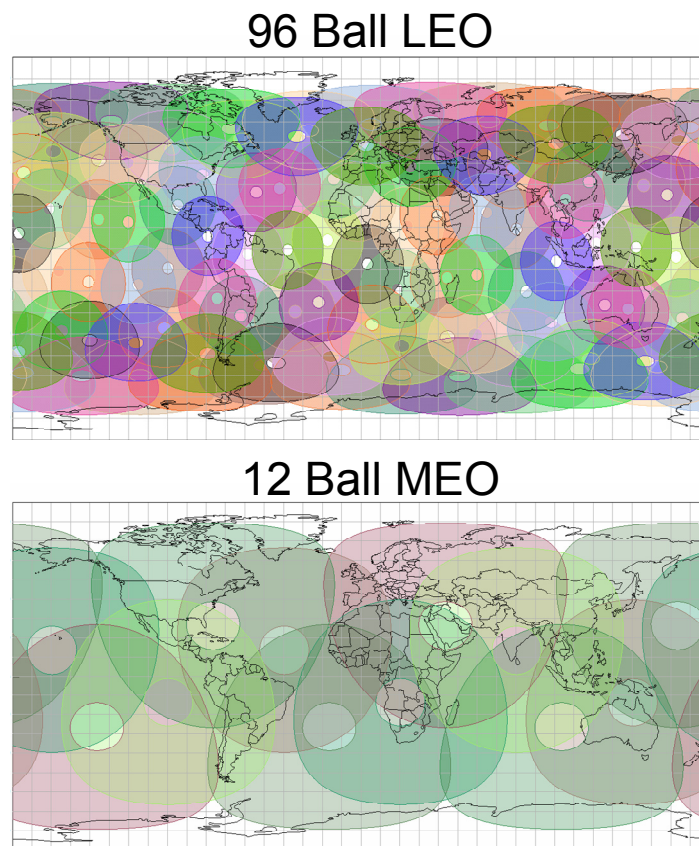


Figure 11: SBR Coverage in MEO vs. LEO (32)

One of the experimental demonstrations of ISAT is to deploy, control and calibrate the large rigidizable structure and verify the deployment process within set tolerances. This will provide extremely useful information for a 300-meter version. Some of these requirements are: the final rigid structure length is within $\pm 3\text{cm}$, structural modes $< 0.5\text{ Hz}$, and beam pointing accuracy $< 10\text{ mrad}$.

If the rigidizable structure meets the standards predicted, it will provide enormous support for the inflatable-rigidizable technology advocates and will become a proven technology. Dr. Michael Zatman, ISAT Program Manager, has also expressed interest in the results from RIGEX (31) along with Dr. Spanjers of DSX.

Space Experiment Review Board (SERB) / Space Test Program (STP)

The Air Force and DoD SERB meet annually to discuss proposed experimental missions, primarily evaluating them on military relevance. Most participants compete for a ‘free ride’ on the Space Shuttle or on an Expendable Launch Vehicle (ELV) as a dedicated or ‘piggyback’ payload, although there is the option of reimbursable flight. If a high ranking is achieved at the DoD SERB, manifestation will be attempted by STP (Figure 12). Manifestation and launch costs are provided by STP.

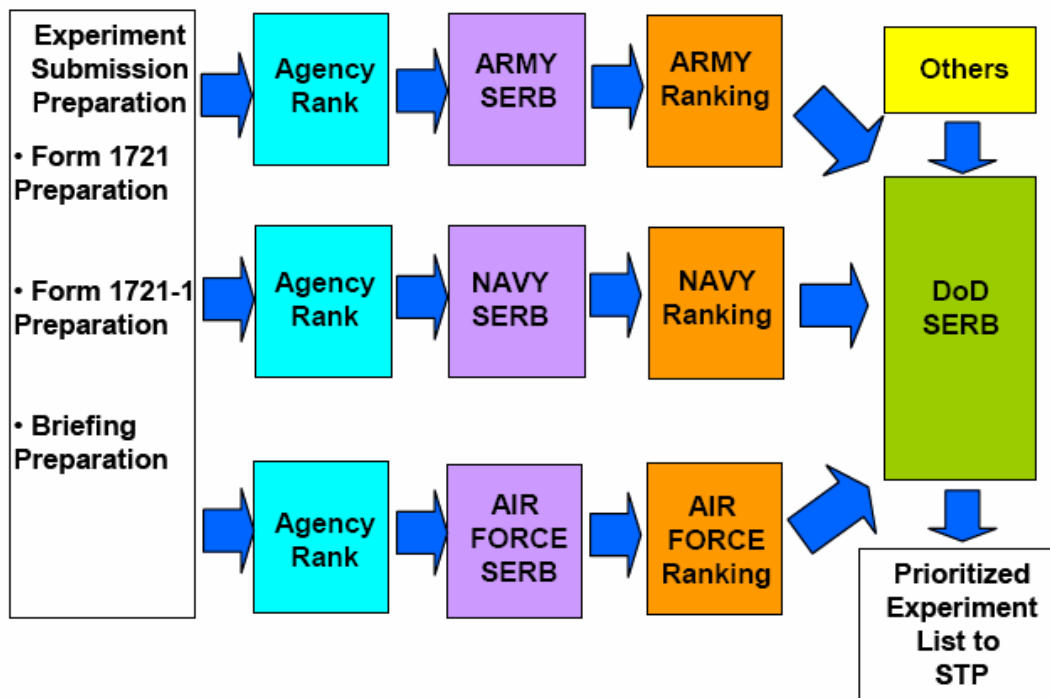


Figure 12: The SERB Process (27)

STP is a DoD activity under Air Force executive management which provides spaceflight for the entire DoD space science and technology community (27). The typical mission life cycle consists of three basic phases: mission design, mission development, and mission execution. Figure 13 shows a sample life-cycle for an STP mission.



Figure 13: STP Mission Life Cycle Activities (27)

As of the 2004 DoD SERB, RIGEX was ranked #26 out of 34 submittals. Even with the lower ranking, RIGEX is currently slated to launch on Space Shuttle mission STS-120 in February 2007. This is due to the small-scale of RIGEX and the fact that it is designed to fit in a standard payload envelope (see next section). All manner of projects compete for manifestation at the SERB, no matter their cost, size, or whether they are full-scale missions; hence the higher ranking of these projects relative to RIGEX.

Payload Envelope

RIGEX was originally designed to fit into NASA's Get-Away-Special (GAS) container (Figure 14) (7). The size, shape, volume and mass of the experiment were all designed around the GAS specifications. During the 2004-2005 timeframe, NASA decommissioned the GAS system in favor of a larger, more flexible system, the Container-for-All-Payload-Ejections (CAPE) (Figure 15).

CAPE was primarily developed as a hardware ejection system with electrical and mechanical interfaces for the payload (4). RIGEX was not designed to be ejected and will therefore mount directly to either the top or bottom plate of the CAPE canister. This new payload envelope has the potential of benefiting RIGEX by increasing the allowable size and weight specifications (Table 4).

Table 4: Comparison of Payload Envelopes

Maximum Allowable Specification	GAS Container (7)	CAPE Canister (4)	Percent Increase
Weight (lb _f)	200	350	175%
Dimensions (in)/ Total Volume (in ³)	19.75 (dia) × 28.25 (ht) 8,655	21.0 (dia) × 53.0 (ht) 18,357	212%

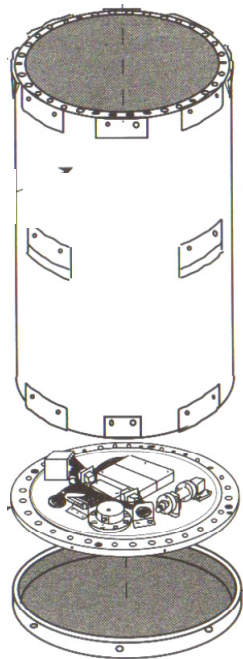


Figure 14: GAS Container

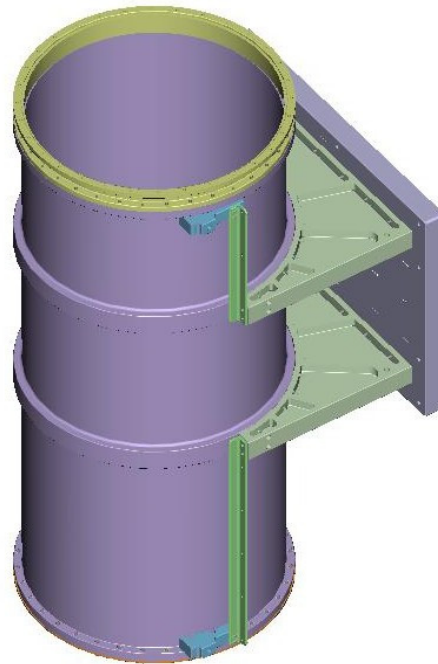


Figure 15: CAPE Canister

RIGEX Power Supply

During a teleconference with the DoD Payloads Office at the Johnson Space Center (JSC) (1), an offer was made by JSC personnel to run RIGEX on Shuttle power instead of batteries. RIGEX was originally designed to use eight stacks of 40 D-cell batteries to run the experiment (Figure 16). This was because relying on Shuttle power lessened the odds of getting a ride; Shuttle-powered slots were rare in the GAS configuration (18).

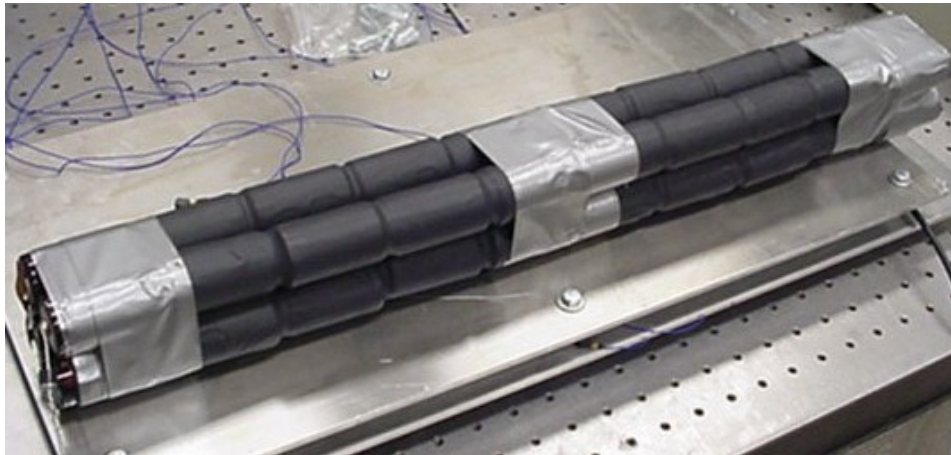


Figure 16: One of Eight Battery Packs Used to Power RIGEX

The decision was made to utilize the Shuttle power option due to the many advantages it offered over RIGEX's internal battery supply. Shuttle power would increase probability of mission success due to the lack of experiment dependency on the limited-life of the batteries. The possibility of a 90-day delay between experiment integration and launch could potentially cause enough battery power loss to cause mission failure. Combine this with the decrease in power at cold extremes and the

increased need for tube heating at these extremes, the battery power could become a major constraint in the RIGEX design. Using Shuttle power also mitigates any safety concerns and regulations imposed by NASA on using batteries. Without the batteries, the weight of RIGEX will drop approximately 55 lbs and free up a large volume of useable space in the center of the main structure. This, in turn, will allow the use of much larger pressure vessels to contain the inflation gas. This will be covered in Chapter III, as a primary contribution of this thesis.

Current Status of RIGEX

The current status of RIGEX going into this thesis is listed below in Table 5. Adjustments will be required for the PC-104 computer (programming, power supply), therefore, the associated software needs to be modified and tested before the system can be finalized. The inflation system will need modification from its previous state. The main structure will need to be modified to accommodate the upgraded inflation system and for changes imposed by NASA, therefore, an updated prototype needs to be fabricated and tested before finalization.

Table 5: Status of RIGEX before Current Thesis Work

Component	Initial Design	Prototyped	Tested	Finalized
Heater Box	✓	✓	✓	✓
Pin-Puller/Latch	✓	✓	✓	✓
Image System	✓	✓	✓	✓
PC-104 Computer	✓	✓		
Inflation System	✓			
Piezoelectric Actuators	✓	✓	✓	✓
Accelerometers	✓	✓	✓	✓
Main Structure	✓			

Chapter Summary

This chapter covered the current and historical research in inflatable and inflatable-rigidizable technology. The procedures of gaining a Shuttle flight were discussed as was the current state of RIGEX in this process. Modifications to RIGEX due to recent changes in the payload enclosure and power supply were also discussed.

Overall, research into inflatable-rigidizable structures and the materials they are comprised of is expanding at a rapid rate. This technology holds much promise for producing very large-scale structures that were previously too large or complex for our current launch capabilities. RIGEX will seek to provide vital information on the performance of inflatable-rigidizables in the space environment, and to add its input to the ever-expanding database of information in the engineering and scientific communities.

III. Methodology

Chapter Overview

This chapter details the methodology, set-up procedures and testing of various RIGEX components. A redesigned pressure system is introduced to alleviate issues with the previous design. Also presented is an analysis of the sub-Tg tubes to characterize their cooling profiles. The information gained from these investigations will provide RIGEX with better overall system performance and therefore improve probability of experiment success on orbit.

Experiment Assembly

Both the pressurization and thermal tests were performed using the prototype quarter structure. This structure represents one bay of the full RIGEX supporting structure. It was designed so it would fit into the vacuum chamber located inside AFIT's vibration laboratory in Bldg 644. All testing, with the exception of basic function checks, was performed inside the vacuum chamber to better simulate the lack of pressure in the orbital environment.

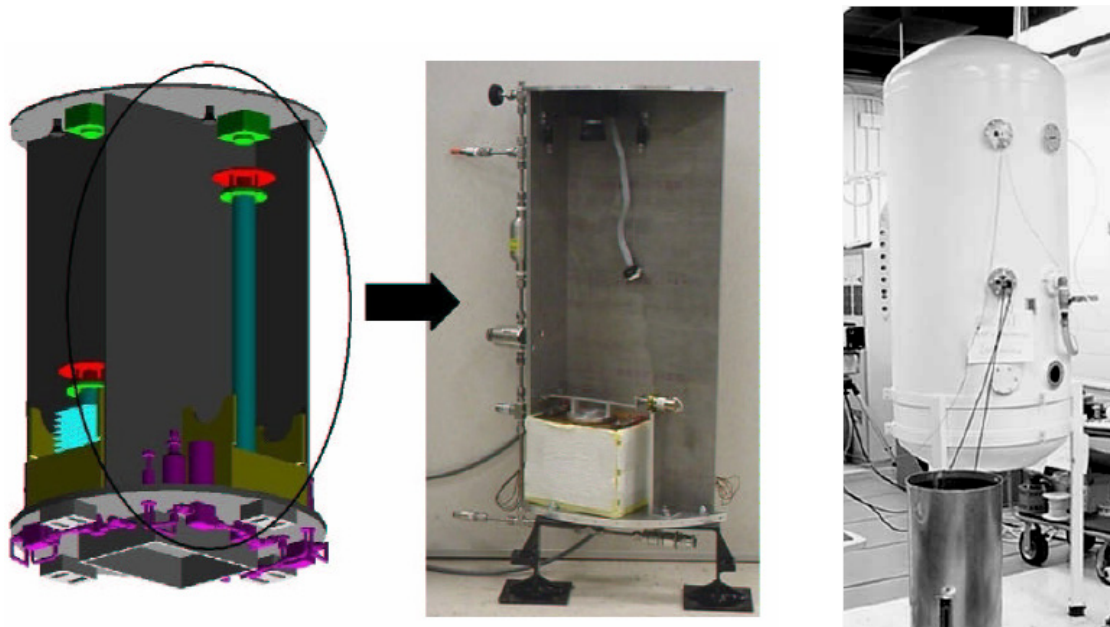


Figure 17: Quarter Structure and Vacuum Chamber

Inflation Tests

As discussed in Lindemuth's thesis (14), the original pressurization system needed modification. Problems were encountered with various components, primarily due to the relatively high pressure of the system. The original system also contained several components increasing the complexity and decreasing the reliability of the entire pressurization subsystem. The many components were necessary to deal with a pressure of 400 psi. The high pressure was needed because the pressure vessels had to be small, 50 cm^3 , due to both a lack of area on the surface of the main structure and the maximum weight allowable in the GAS system. The problem with so many components is that the addition of each adds two to three more possible leak points where the system could lose pressure.

The desired inflation pressure is 4 psia (10 psia maximum) for proper deployment of the tube. Overpressure could damage the tube in the softened state, especially during heating. The original solenoid chosen, nor the tube itself, could deal directly with the 400 psi from the pressure vessel; therefore a regulator to limit the gas flow rate was necessary. The original system also contained a pressure-relief valve to vent the gas after tube rigidization and to prevent overpressure. A two-way solenoid was eventually chosen that made the pressure-relief valve unnecessary. One recommendation from Lindemuth's thesis stated:

A final improvement for the inflation system would be to increase the volume in the pressure vessel that feeds the inflation system. With a large enough bottle, the system could function successfully even if the pressurized portion of the system equalized with atmospheric pressure before mission launch. (14)

With this single improvement, two of the components could be eliminated. The regulator would no longer be needed to slow down flow to the solenoid, considering the entire pressurized system during tube deployment would be 8.4 psia maximum. The fill-valve could also be eliminated. Simply removing the pressure transducer on the ground for a few moments and then reinstalling it would be enough to 'pressurize' the system to 14.7 psia.

This improvement also negates the possibility of the system losing pressure on the pad while waiting for launch, which could be up to 90 days. Should there be a small leak, the system will equalize with the atmosphere and therefore does not need monitoring. At Cape Canaveral, which is at sea level and is the location for Shuttle launch, the atmospheric pressure would be the required 14.7 psia.

As discussed in Chapter II, NASA JSC specified the use of Shuttle power, therefore allowing RIGEX to be relieved of its battery-powered requirement. This change left the RIGEX main structure with a large useable volume (8.5" × 6.25" × 28.0") where the batteries were originally to be mounted (Figure 18).

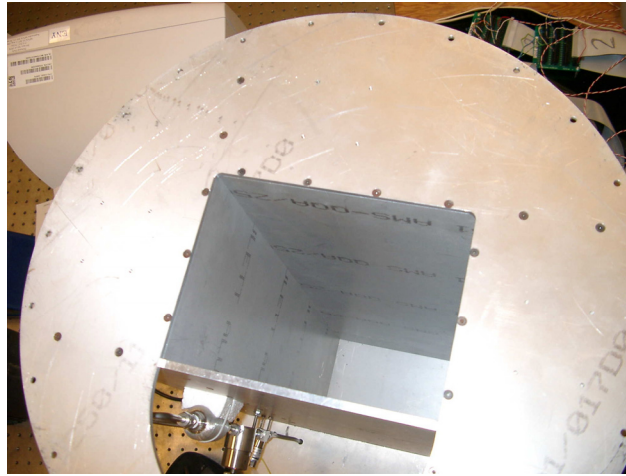


Figure 18: Battery Storage Volume

The larger pressure vessels suggested by Lindemuth could be mounted in this volume. The original pressurization system incorporated vessels which would only hold 50 cm³ of gas. To contain enough moles to inflate the tubes, the vessels held the gas at 400 psia. These vessels were required due to the lack of useable surface area for mounting larger vessels and the weight restriction on the original GAS container, which was 200 lb_f.

The sub-Tg tubes used in RIGEX must have an inflation pressure between 4 psia and 10 psia. 4 psia is the minimum pressure required to force out the tubes' residual

stresses. These stresses are caused by the folds of the graphite/epoxy and thermoset plastic the tubes consist of. 10 psia is the maximum allowable tube pressure before potential failure; the tubes themselves or the adhesive attaching the aluminum endcaps to the tube could fail and potentially cause a hazardous situation.

Considering the changing constraints and the desire to increase reliability and reduce risk, an analysis was performed to determine what size pressure vessel could be used to maintain atmospheric pressure and still contain enough gas to fully inflate the tubes in the vacuum of space.

Pressure Vessel Volume Determination

Using the above pressure requirements, an analysis was accomplished to find what size pressure vessel would allow full inflation within the 4 to 10 psia constraints and be maintained at atmospheric pressure, 14.7 psia (0 psig).

To accurately calculate the volume of the new pressurization system, a layout for the system had to be conceived to obtain the length of tubing used. Even though the amount of gas contained in the tubing and small components is relatively minute relative to the pressure vessel, the sum of their respective volumes was taken into account to increase the accuracy of the calculations. Depending on the size pressure vessel chosen, the length of tubing will vary (Figure 19). Different pressure vessels have different lengths associated with them; therefore the tubing opposite the pressure vessel will change length due to the geometry of the system layout.

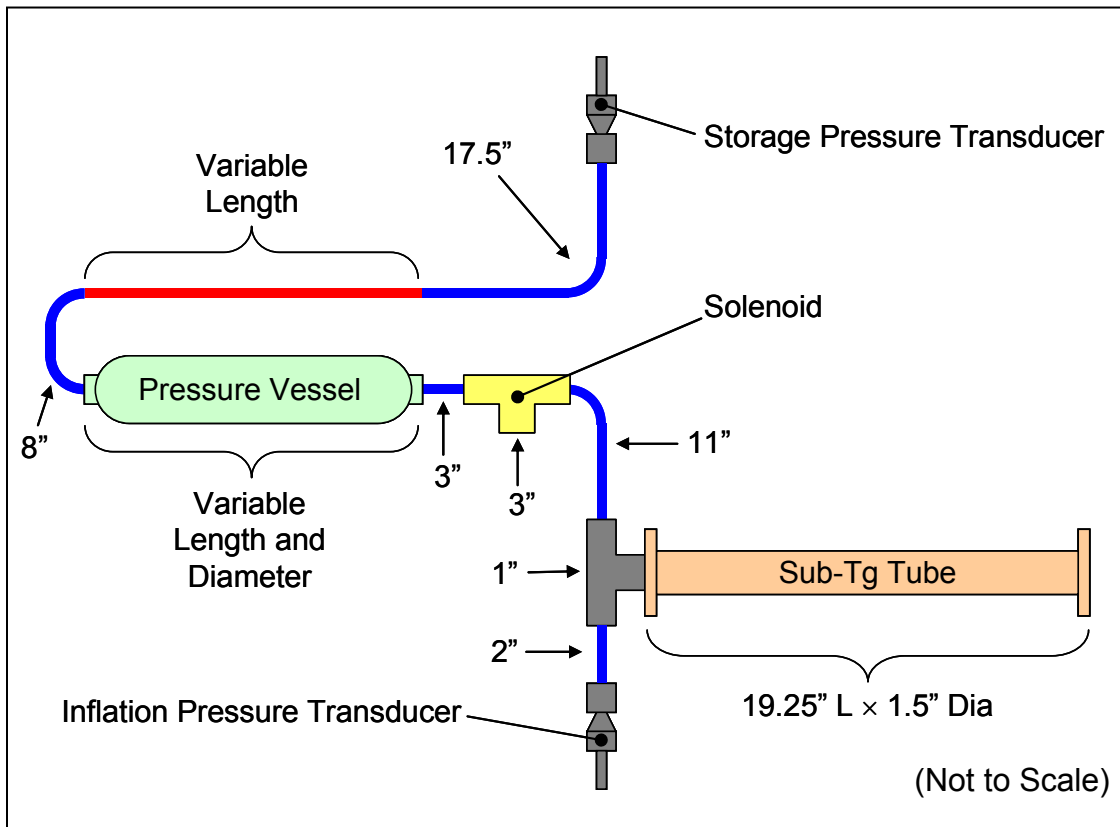


Figure 19: Pressure System Layout

There are two primary sections of the modified pressurization system (Figure 20). The first is the storage section. This section contains the tubing leading from the pressure transducer at the fill point to the pressure vessel, the vessel itself, and the tubing leading up to the solenoid's built-in valve. The second part of the system, the inflation section, consists of the tubing leading from the solenoid's built-in valve to the sub-Tg tube, the tube itself, and the tubing from the tube to the final pressure transducer.

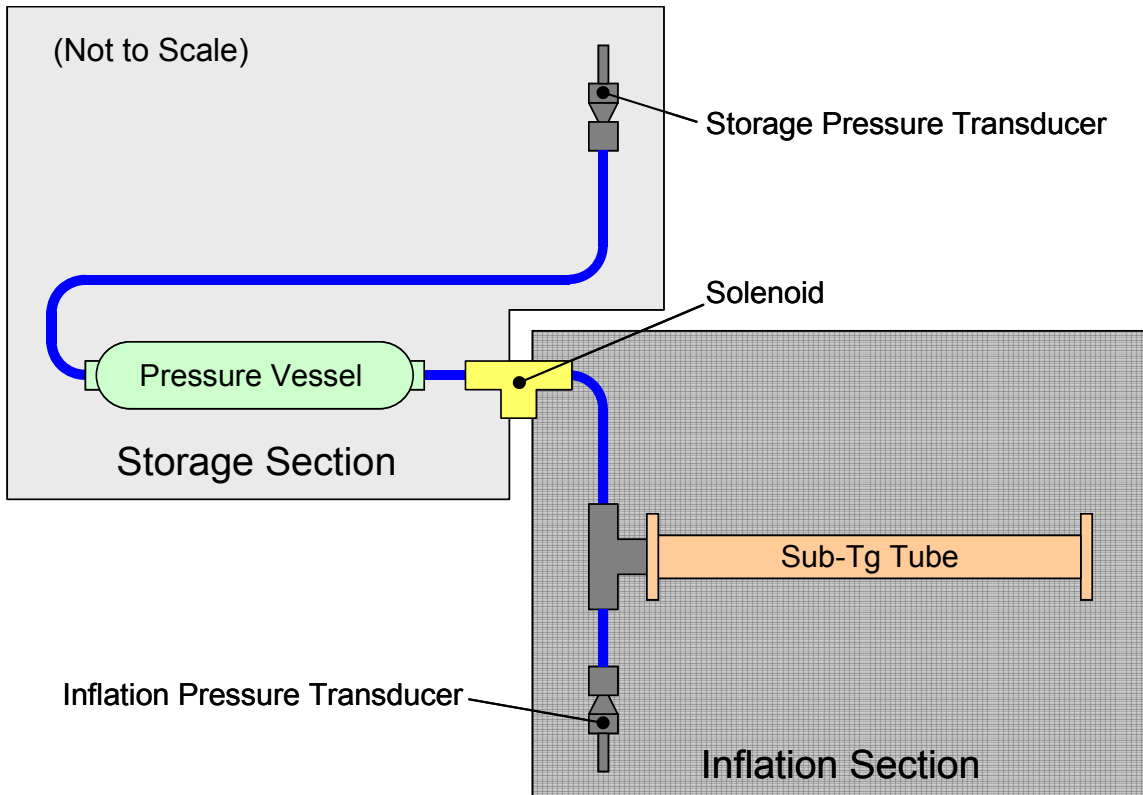


Figure 20: Pressure System Breakdown

The inflation section's volume is fixed because it is sealed off from the storage section by the solenoid valve; therefore its total volume is known. Knowing this fixed volume, the total system volume could be determined by solving for the necessary number of moles of gas to create a final system pressure within the pressure constraints.

Since the number of moles in the storage section will equal the number of moles in the entire system once the solenoid is open (conservation of mass), and since either air or nitrogen will be used, the perfect gas law (Eq. 1) can be applied:

$$P \cdot V = n \cdot R \cdot T \quad (1)$$

where

$P = \text{pressure (torr)}$

$V = \text{volume (cm}^3\text{)}$

$n = \text{number of moles (mol)}$

$R = \text{gas constant (L} \cdot \text{torr/mol} \cdot \text{K)}$

Using Swagelok's[®] inventory of pressure vessels for the volume and length specifications, the combined gas law (Eq. 2) was derived (Eq. 3) to solve for the final pressure ranges. Each vessel will have a range due to the changes in the survival temperature in orbit (−60°C to 85°C):

$$\frac{P_1 \cdot V_1}{T_1} = \frac{P_2 \cdot V_2}{T_2} \quad (2)$$

where

$P_1 = \text{storage section pressure (psia)}$

$P_2 = \text{total system pressure (psia)}$

$V_1 = \text{storage section volume (cm}^3\text{)}$

$V_2 = \text{total system volume (cm}^3\text{)}$

$T_1 = \text{gas temperature when stored (K)}$

$T_2 = \text{survival temperature (K)}$

therefore

$$P_2 = \frac{P_1 \cdot V_1 \cdot T_2}{V_2 \cdot T_1} \quad (3)$$

Swagelok offers several sizes of pressure vessels. Each meets the minimum DOT-3A or 3E 1800 psig certification NASA requires. The results of the analysis came from matching a vessel from Swagelok's product line to the requirements. Due to the inner dimensions of the battery box, two secondary constraints were the length and diameter of the pressure vessels. If either of these dimensions were too great, there would not be enough space in the battery box to contain all three vessels plus tubing.

The calculated results revealed that either the 400cm³ or 500cm³ pressure vessel would fulfill the system requirements (Table 6).

Table 6: Total System Pressures and Vessel Dimensions*

Vessel Size (cm ³)	Low Pressure (psia)	High Pressure (psia)	Diameter (in.)	Length (in.)	Practicability
150	2.376	3.992	2.00	5.25	Outside Range
300	3.761	6.320	2.00	8.94	Outside Range
400	4.448	7.473	2.00	11.4	Inside Range
500	5.006	8.411	2.00	13.8	Inside Range
1000	6.717	11.287	3.50	10.9	Outside Range
2250	8.362	14.051	3.50	17.2	Outside Range

* Available sizes meeting NASA requirements.

The 500cm³ vessel (Figure 21) was chosen because of its larger capacity. If a small pressure leak were to develop between launch and scheduled tube inflation, the 500cm³ vessel would provide a larger margin of safety of gas to compensate.



Figure 21: Size Comparison of 50cm³ vs. 500cm³ Vessel

The modified system appeared promising. As expected, it offered several advantages over the previous system (Table 7). Again, with this design, if there were a small leak in the system prior to launch, the system will equalize with atmospheric pressure. The system was constructed and testing commenced.

Table 7: Original vs. Modified Pressurization System

Element	Original	Modified	Comments
Pressure of Gas (psia)	400	14.7	Higher Safety/Higher Reliability
Major Components	5	3	Less Complexity/Higher Reliability
Possible Leak Points	18	12	Higher Reliability

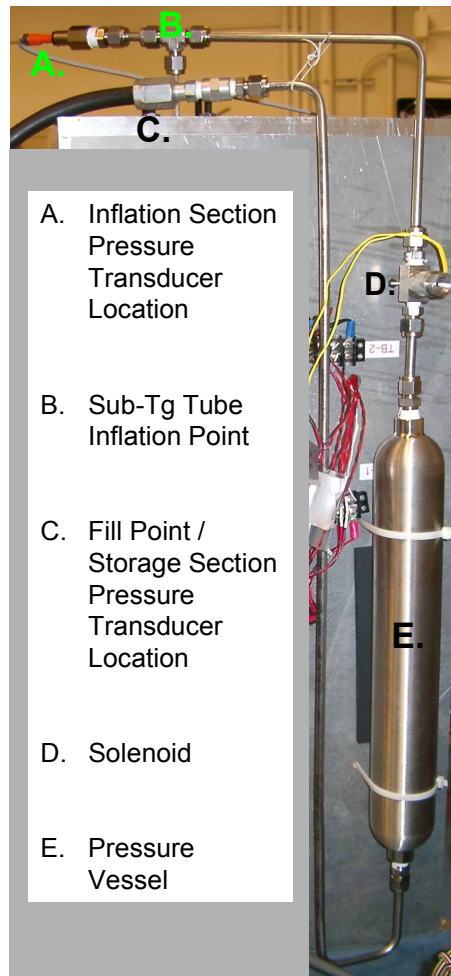


Figure 22: Redesigned Pressure System

Inflation Test Setup and Procedures

The first pressurization test was done using a cloth tube (Figure 23). The dimensions are the same as the sub-Tg tubes; therefore the amount of gas needed to inflate the cloth tube's volume was the same. All tests following the cloth tube test were performed on sub-Tg tubes.

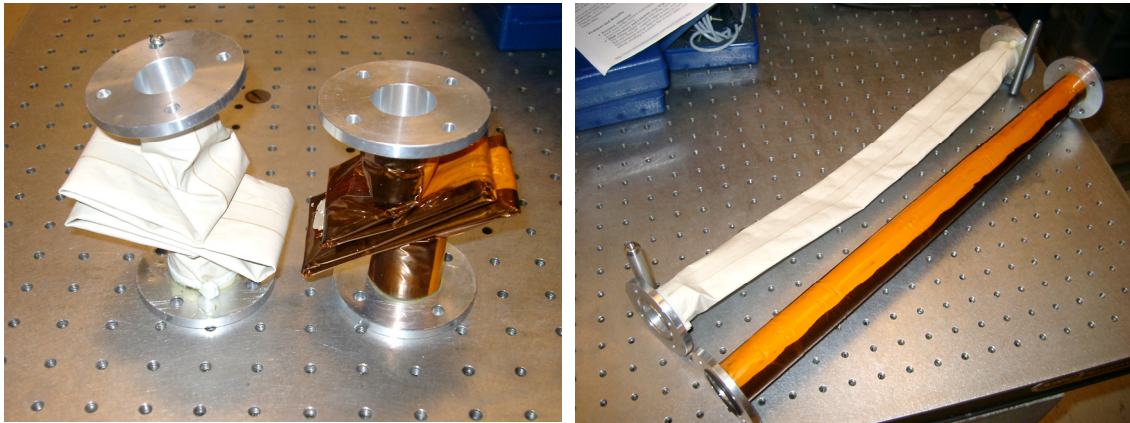


Figure 23: Cloth and Sub-Tg Tubes

The solenoid which separates the two sections of the system is closed without power. This keeps the storage section of the pressure system sealed. Also, when closed, the solenoid leaves the inflation section of the system open to the environment, maintaining equalization with the external pressure (Figure 24). This is a requirement to avoid having the tubes pressurize during ascent after launch.

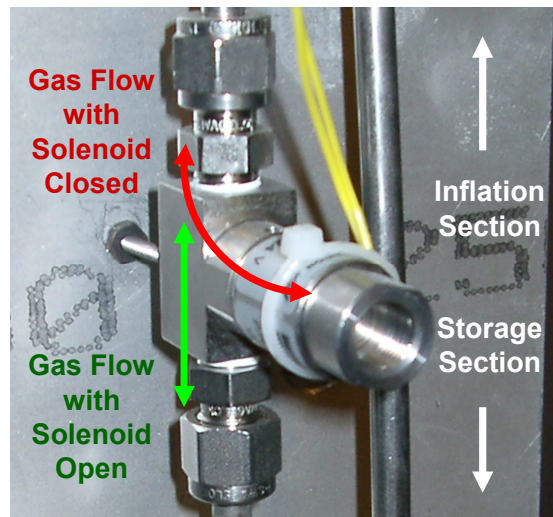


Figure 24: Solenoid Operation

If the inflation section were sealed, the small amount of gas contained within it at atmospheric pressure could potentially cause a failure in the folded, rigid tube. This is due to the increased pressure it would experience in the vacuum of space. Also, since the tubes will be vented of their gas after rigidization, a vacuum will exist inside the tube in space. Should the tube be closed off from the environment during reentry, it could potentially be crushed under atmospheric pressure during descent.

The pressure transducers used had useful ranges up to 15 psia and 15 psig. These were the only two available to test with. Preferentially, and for the final flight article, both should be absolute gauges, given that the gauge pressure transducer's reference changes depending on its surrounding environment.

The vacuum chamber did not create a perfect vacuum. The closest approach was 0.30 psia. At this chamber pressure, however, there was still plenty of pressure in the storage section to fully deploy sub-Tg tubes and run valid tests. Also, the chamber held pressure relatively well. Over the roughly 10,000 seconds of total time recorded for each test, the maximum pressure loss was only 0.07 psia.

The pressure system itself is constructed of stainless-steel tubing and components, with the exception of a small piece of plastic tubing connecting the system to the heater box, which is in turn bolted to the tube. This connection has been improved in the final support structure design, which has threaded connections directly through the aluminum structure into the sub-Tg tubes.

A description of the pressure tests conducted, along with the results from the pressure tests are presented in Chapter IV.

Thermal Tests

The heater boxes are required to bring the sub-T_g tubes up to their glass-transition temperature. Once the experiment sequence is activated, the heater boxes warm the tubes by way of Minco Thermofoil™ (17) resistive heaters mounted to the interior walls of the boxes (Figure 25). Each box is composed of a 0.25 inch thick Ultem 1000, PEI, Polyetherimide plastic shell (21), the resistive heaters surrounded by adhesive-backed foil, and compressed fiberglass insulation on the exterior.

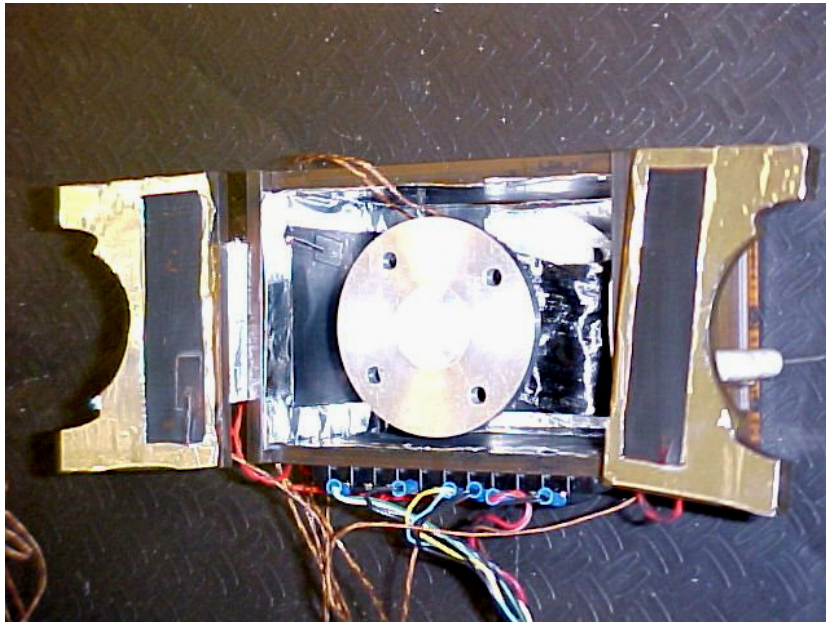


Figure 25: Heater Box Composition

Each heater box contains eight Minco heaters. The flat black painted side of the patch radiates into the heater box; while the foil-covered side is adhered to the box itself (Figure 26). These two features increase radiation into the box and decrease heat loss out of the box.

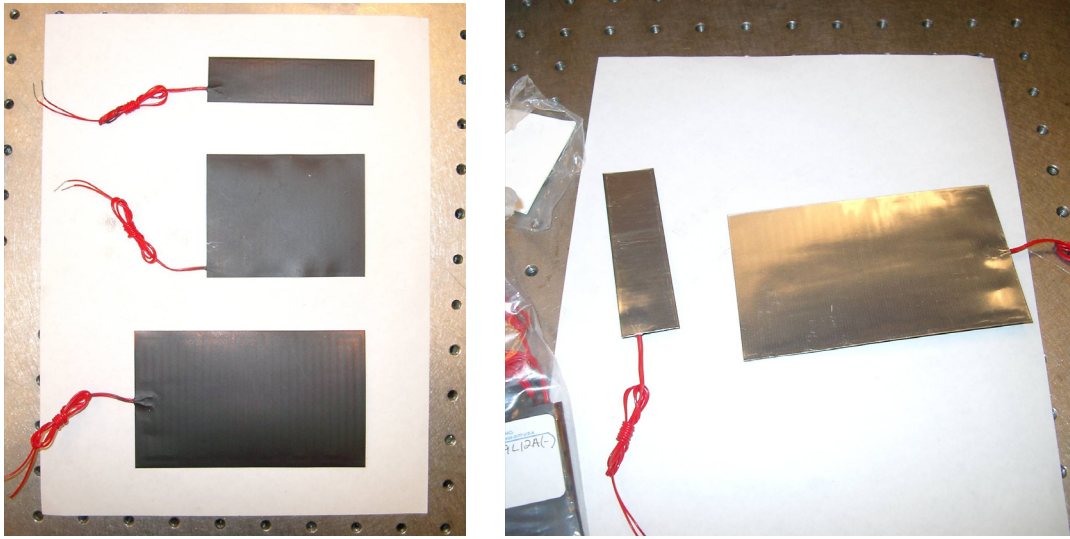


Figure 26: Minco Thermofoil™ Resistive Heaters

The heater patches are wired into three circuits inside the heater boxes. These circuits produce predetermined resistances (21). The values from previous research measured for each Thermofoil™ heater resistance differed from those found during testing. The observed resistances are compared to the original values in Table 8. Since the overall resistance-per-set of heater patches was relatively close, they were wired in the same way as the original specifications stated (21). These circuits are shown in Figure 27.

Table 8: Minco Thermofoil™ Heater Resistances

Heater Location	Number	Specified Resistance (Ω)	Specified Resistance per Set (Ω)	As-Tested Resistance (Ω)	As-Tested Resistance per Set (Ω)
Top Left	1	9.5	9.5	8.9	8.9
Top Right	2	9.5		8.9	
Bottom Left	3	9.5		8.9	
Bottom Right	4	9.5		8.9	
Left Side	5	27.3	13.65	21.9	10.95
Right Side	6	27.3		21.9	
Front	7	11.3	22.6	10.3	20.6
Back	8	11.3		10.3	

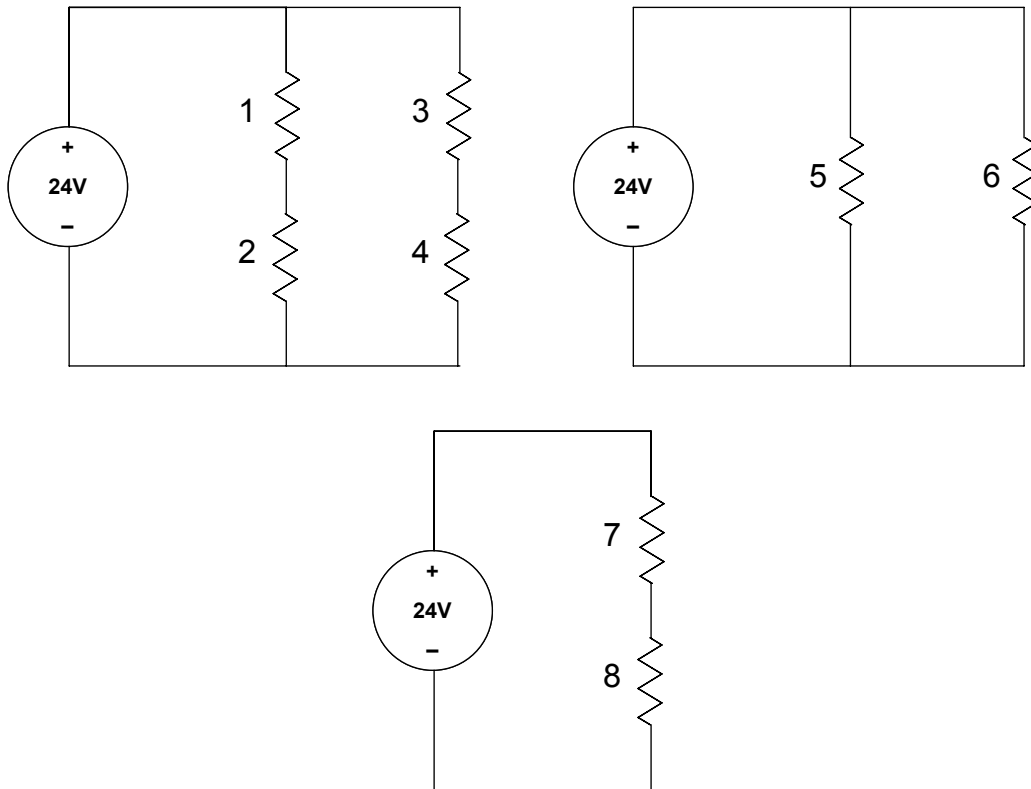


Figure 27: Resistive Heater Wiring Diagrams (21)

The heating profile of the sub-Tg tubes was investigated by Philley (21) and Lindemuth (14). Philley examined the lower three inches of the tubes. This test, however, did not provide enough assurance that the entire tube had reached the transition temperature, 125°C. Because of this, Lindemuth experimentally determined the heating differential across the entire tube to determine the slowest-heating portion. He found that fold #2 (Figures 28 and 29) heated the slowest. This is due to the fact that this location is most protected from the direct radiation the resistive heaters produce. This location was used in the current tests to track when the entire tube had reached 125°C.

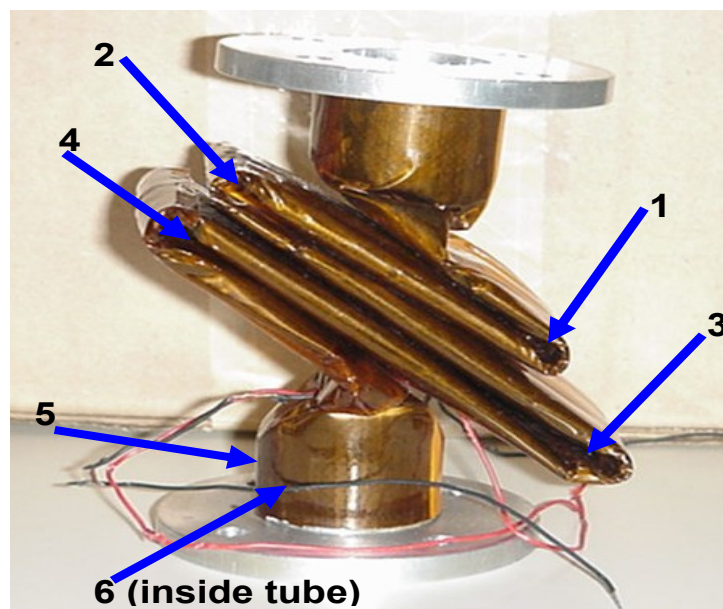


Figure 28: Thermocouple Locations for Heating Differential Test (14)

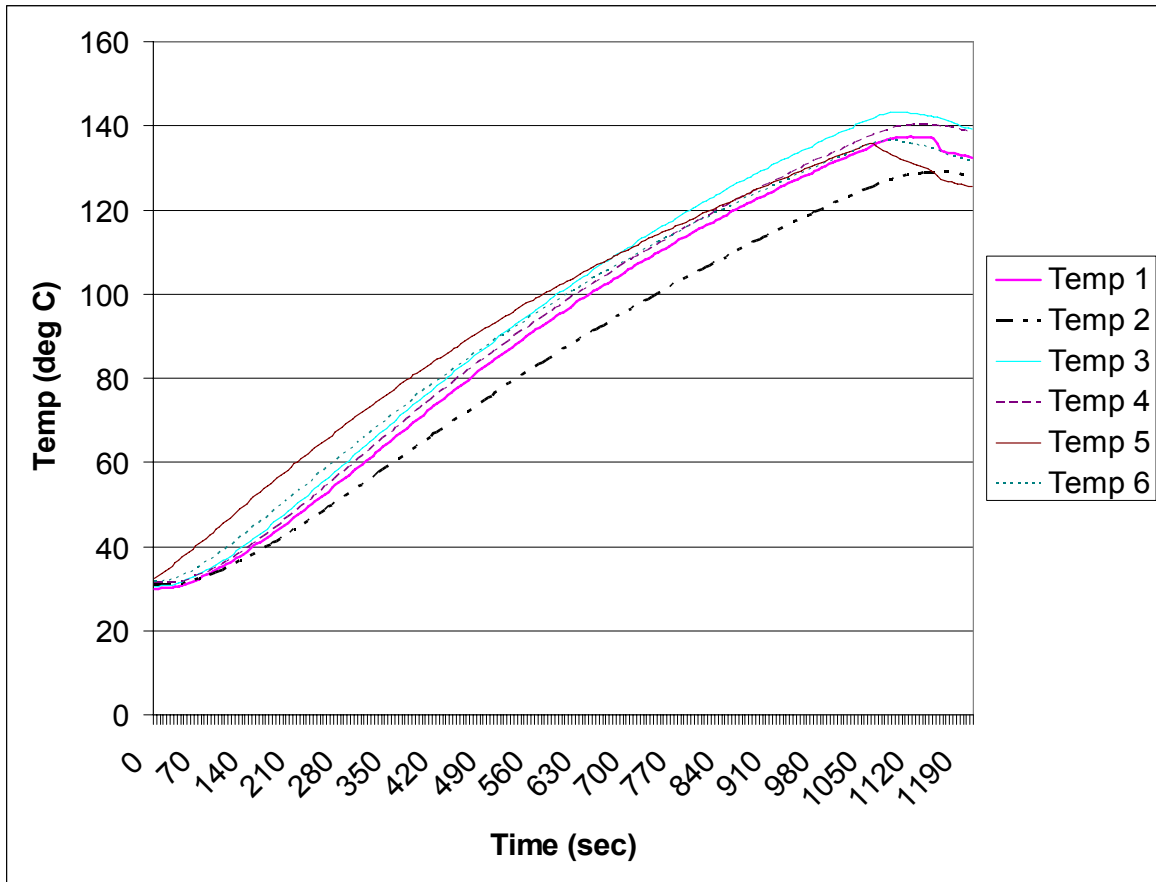


Figure 29: Heating Differential Across the Tube (14)

Even though the slowest-heating location on the tube had been found, the fastest-heating was not determined. The fastest-heating location is important to know because this is the section of the tube which will cool the slowest. All areas of the tube need to be well below 125°C before the tube is vented. The end-cap locations do not heat as quickly due to the large mass of material involved. Philley recorded a 52°C difference between the two thermocouple locations he used, with the lower temperature thermocouple mounted on the portion of the tube covering the aluminum end-cap.

Due to the fact that fold #3 reached the highest temperature during Lindemuth's testing, it was assumed that the fastest-heating location was on the external portion of this fold. This location is closest on the folded tube to one of the resistive heaters. Therefore, the two locations used to evaluate the cooling profile for maximum and minimum temperatures were inside fold #2 and outside fold #3. For the current tests, these locations were renamed #1 and #2, respectively (Figure 30).

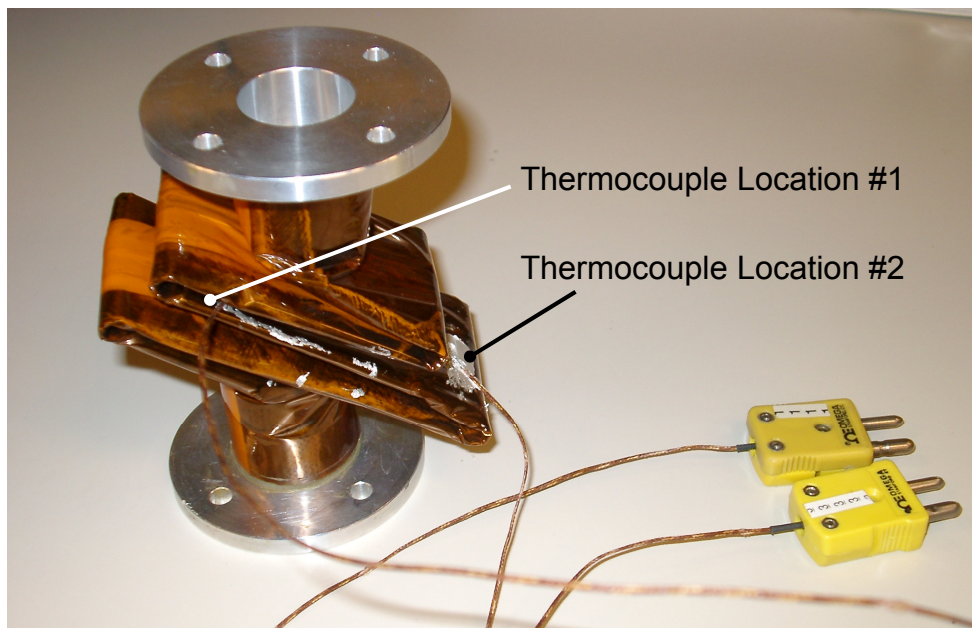


Figure 30: Cooling Profile Thermocouple Locations

Although the heating profile of the tubes was performed, a cooling profile was not accomplished. The cooling profile is important for two reasons. First, the tubes must drop below their glass-transition temperature, 125°C, before they rigidize. Once a tube is rigidized, the pressurized gas contained within can be vented. Early venting, before the

tube is fully cooled, may affect the deployed state and should be avoided. The second reason the cooling profile is important is because the piezoelectric patches that excite the tubes must be at 66°C or below to be within their optimal operating range (26). Non-optimal results were returned when the patches were activated above this temperature. The high temperature was thought to be the cause (18), thus a ‘cooling time’ to include in the software is desired for proper performance of the experiment.

Cooling Profile Determination

Calculations were performed to validate the cooling profile of the tubes. An equation was sought to find the time for a sub-T_g tube to cool given an initial temperature (temperature at deployment) and an ambient temperature. Cooling primarily by radiation was taken in account. Since the experiments were run in a near-vacuum environment, as will be the case on orbit, cooling by convection was considered negligible and therefore disregarded. Even before the tube is vented, the air inside loses very little heat through convection due to air’s inherently low heat transfer properties. Cooling by conduction was also considered relatively small as compared to radiation, though not as insignificant as convection.

A simplified figure of the test set-up is shown in Figure 31. Unfortunately, the temperatures of the adjoining plates (locations #2 and #3) surrounding the tube on the aluminum quarter-structure were not recorded during testing. Without these values, calculating the heat transfer rate by radiation could not be accomplished without using gross assumptions for the time-dependent temperature of these plates.

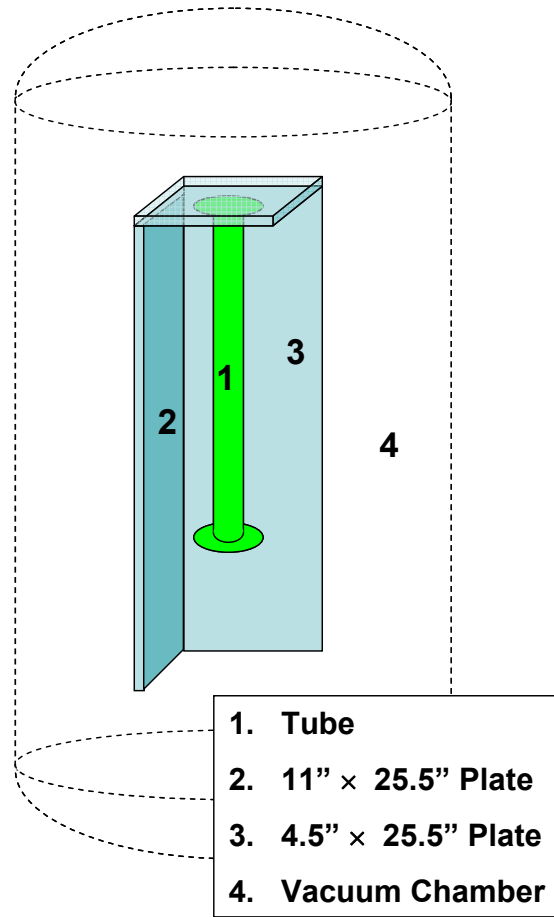


Figure 31: Major Surfaces Involved in Radiation Analysis

Another method of calculating the tube temperature over time was considered. This was the *lumped capacitance method* for radiation (11). This method uses an energy balance based on the initial (highest) temperature, the ambient temperature, and specific material properties of the tube. This energy balance was used because it is assumed that the sub-Tg tube will lose all of its heat \dot{E}_{stored} to its surrounding environment \dot{E}_{out} . The equation derivation is shown below.

Energy balance:

$$\dot{E}_{stored} = -\dot{E}_{out} \quad (4)$$

where

$$\dot{E}_{stored} = \rho V c \frac{dT}{dt} \quad (5)$$

The stored energy is an expression of the tubes' material density ρ , volume V , specific heat c , and temperature gradient over time $\frac{dT}{dt}$. The energy leaving the system:

$$\dot{E}_{out} = \varepsilon \sigma A_s (T^4 - T_{amb}^4), \quad (6)$$

is an expression of the radiative properties of the tube and therefore includes values for emissivity ε , the Stefan-Boltzman constant σ , surface area A_s , and temperature T , T_{amb} .

Substitution gives:

$$\rho V c \frac{dT}{dt} = -\varepsilon \sigma A_s (T^4 - T_{amb}^4) \quad (7)$$

where, as mentioned previously,

$$\dot{E}_{stored} = \text{rate of change of energy stored in system (W)}$$

$$\dot{E}_{out} = \text{rate of change of energy leaving system (W)}$$

$$\rho = \text{material density (kg/m}^3\text{)}$$

$$V = \text{volume of material (m}^3\text{)}$$

$$c = \text{specific heat of material (J/kg}\cdot\text{K)}$$

$$\varepsilon = \text{emissivity of material (unitless)}$$

$\sigma = \text{Stefan-Boltzman constant } (5.670 \times 10^{-8} \text{ W/m}^2 \cdot \text{K}^4)$

$A_s = \text{outer surface area (m}^2\text{)}$

$T = \text{temperature at any given point in time (K)}$

$T_{amb} = \text{ambient temperature (K)}$

Separating variables and integrating from the initial condition to any time t :

$$\frac{\varepsilon \sigma A_s}{\rho V c} \int_0^t dt = \int_{T_i}^T \frac{1}{T_{amb}^4 - T^4} dT \quad (8)$$

where

$T_i = \text{temperature during deployment (K)}$

Evaluating both integrals:

$$\left(\frac{\varepsilon \sigma A_s}{\rho V c} \right) \cdot t \Big|_0^t = \frac{1}{2T_{amb}^3} \left[\frac{1}{2} \cdot \ln \left| \frac{T_{amb} + T}{T_{amb} - T} \right| + \tan^{-1} \left(\frac{T}{T_{amb}} \right) \right] \Big|_{T_i}^T \quad (9)$$

therefore

$$\left(\frac{\varepsilon \sigma A_s}{\rho V c} \right) \cdot t = \frac{1}{2T_{amb}^3} \left[\frac{1}{2} \cdot \ln \left| \frac{T_{amb} + T}{T_{amb} - T} \right| - \frac{1}{2} \cdot \ln \left| \frac{T_{amb} + T_i}{T_{amb} - T_i} \right| + \tan^{-1} \left(\frac{T}{T_{amb}} \right) - \tan^{-1} \left(\frac{T_i}{T_{amb}} \right) \right] \quad (10)$$

Rearranging:

$$t = \frac{\rho V c}{4 \varepsilon A_s \sigma T_{amb}^3} \left\{ \ln \left| \frac{T_{amb} + T}{T_{amb} - T} \right| - \ln \left| \frac{T_{amb} + T_i}{T_{amb} - T_i} \right| + 2 \left[\tan^{-1} \left(\frac{T}{T_{amb}} \right) - \tan^{-1} \left(\frac{T_i}{T_{amb}} \right) \right] \right\} \quad (11)$$

Equation 11 will calculate how long it takes for the tube to reach a given temperature T using the initial temperature during deployment, T_i . Using a 1°C discrete

temperature value in the temperature range between the initial temperature T_i and ambient temperature T_{amb} , the time for the tube to cool to each sequential degree was solved for. This equation, however, cannot be solved explicitly for temperature T given T_{amb} , T_i , and t .

For all calculations, an initial temperature of 170°C was used. It was experimentally shown (Chapter IV) that there is a difference of 25 – 30°C between the hottest and coolest parts of the tubes. For the actual experiment, the heaters will continue to heat the tubes for 600 seconds (10 minutes) after the slowest-heating portion of the tube reaches transition temperature. With the 600 second delay before deployment, the maximum tube temperature observed on the coolest part of the tube was 140°C. Adding a 30°C adjustment to estimate the maximum temperature on the entire tube produced the 170°C value. This will stay relatively constant no matter what the ambient temperature is, since the 600 second delay is based on glass-transition temperature only (125°C).

The sub-Tg tube property constants are shown below in Table 9.

Table 9: Sub-Tg Tube Constants

Property	Constant
ρ	864.307 kg/m ³
V	1.138×10^{-5} m ³
c	700 J/kg·K
ε	0.95
A_s	60.045×10^{-3} m ²
σ	5.670×10^{-8} W/m ² ·K ⁴
T_i	170°C

All properties refer only to the sub-Tg material of the tube, not the aluminum end caps. The density ρ and specific heat c are derived lumped values of the four materials that make up the tubes (8, 9), thermoset plastic, graphite, epoxy, and Kapton. The emissivity ε was derived from experimental results. Actual properties are proprietary; however, the values used provide reasonably accurate predictions of tube cooling as shown in Chapter IV. Material volume V and surface area A_s were directly calculated.

When solved, the solutions to Equation 11 result in units of s/K^3 , instead of *seconds* alone. This is due to a scaling factor, which was calculated against experimental data and found to average $16.625 K^4/K$. This value was used to calibrate the results from the preceding equation to provide a best-fit match the experimental results. Therefore, the actual equation used for analysis was:

$$t = (16.625 K^3) \frac{\rho V c}{4 \varepsilon A_s \sigma T_{amb}^3} \left\{ \ln \left| \frac{T_{amb} + T}{T_{amb} - T} \right| - \ln \left| \frac{T_{amb} + T_i}{T_{amb} - T_i} \right| + 2 \left[\tan^{-1} \left(\frac{T}{T_{amb}} \right) - \tan^{-1} \left(\frac{T_i}{T_{amb}} \right) \right] \right\} \quad (12)$$

The resulting cooling profiles calculated using Equation 12 are shown below in Figures 32 thru 36. They are displayed consecutively by minimum to maximum ambient temperatures, and are plotted on the same time scale (4000 seconds) for direct comparison.

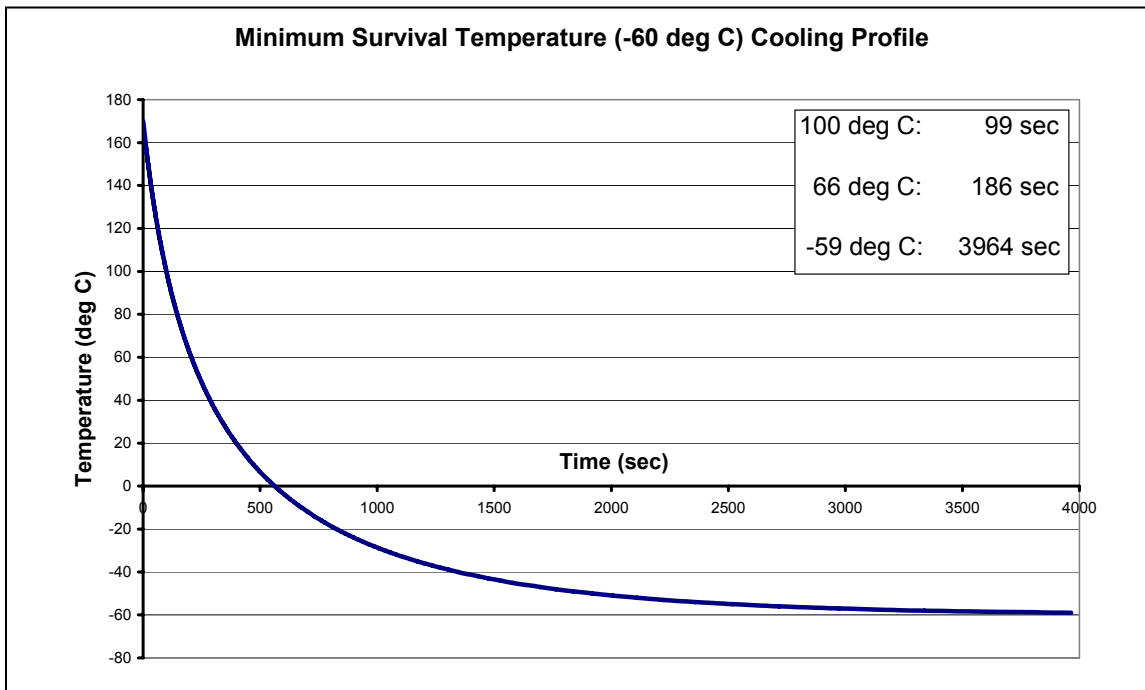


Figure 32: Calculated Sub-Tg Tube Cooling Profile, -60°C Ambient Temperature

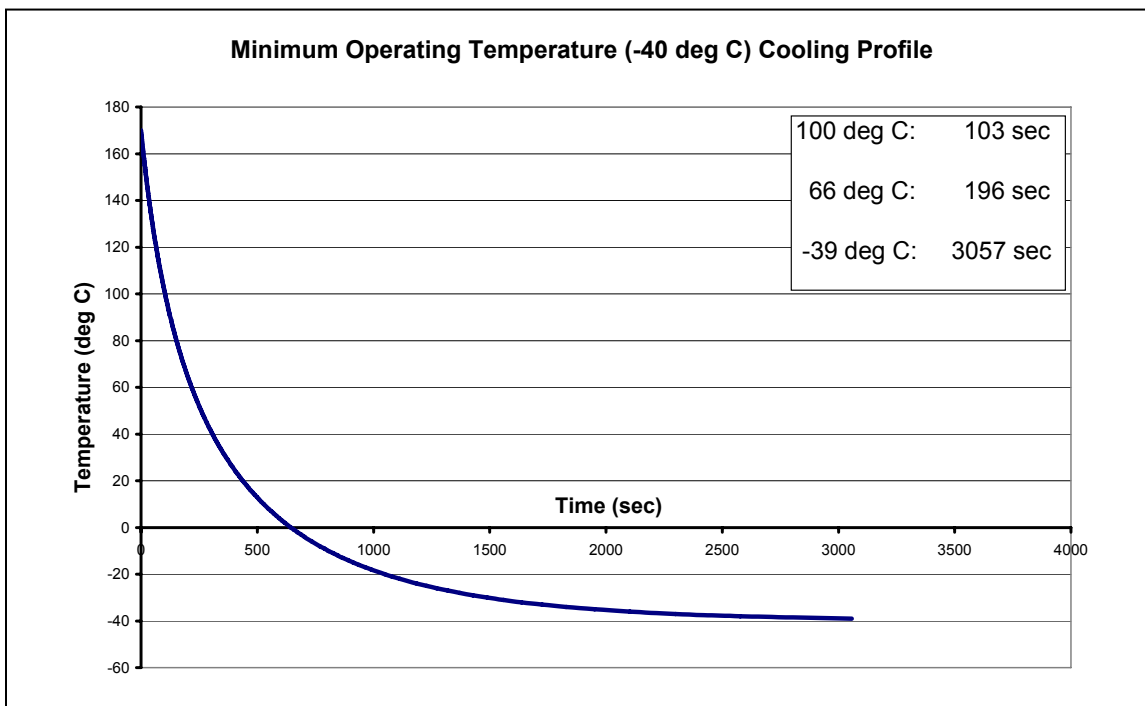


Figure 33: Calculated Sub-Tg Tube Cooling Profile, -40°C Ambient Temperature

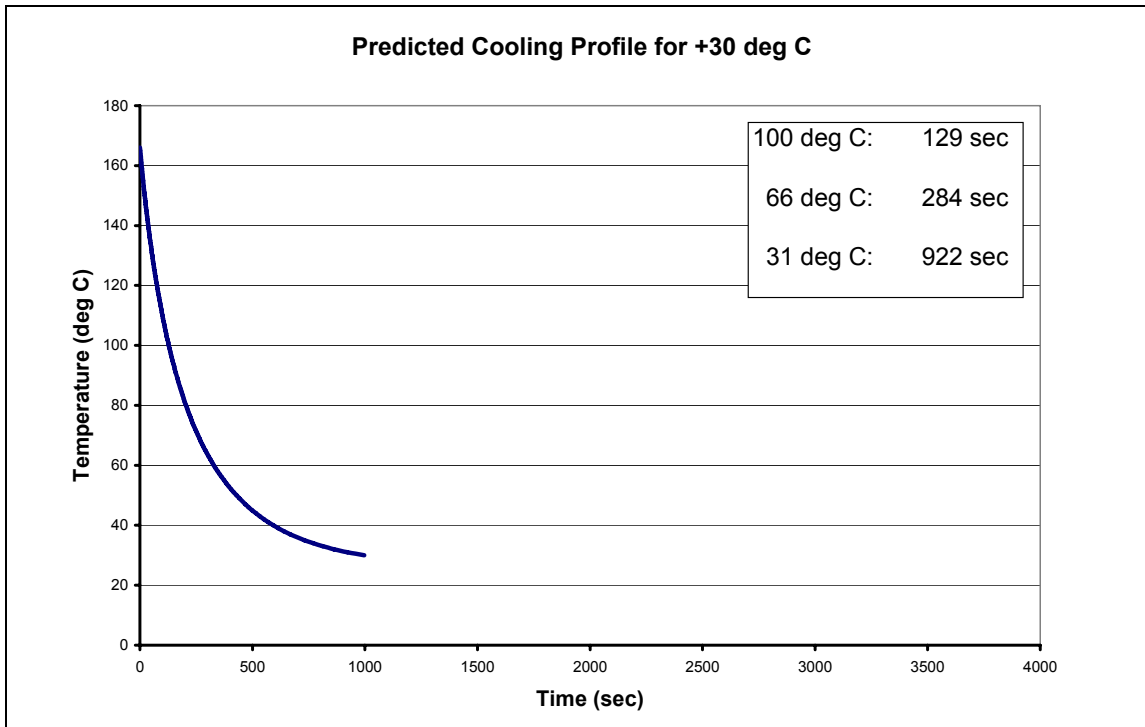


Figure 34: Calculated Sub-Tg Tube Cooling Profile, 30°C Ambient Temperature

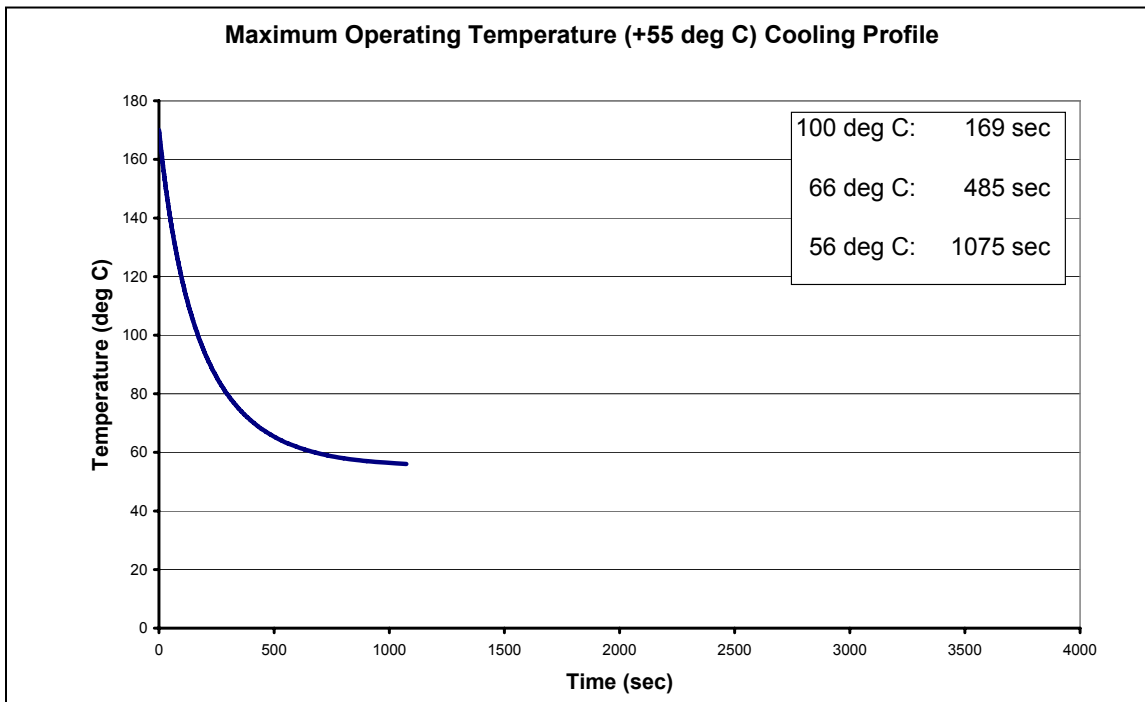


Figure 35: Calculated Sub-Tg Tube Cooling Profile, 55°C Ambient Temperature

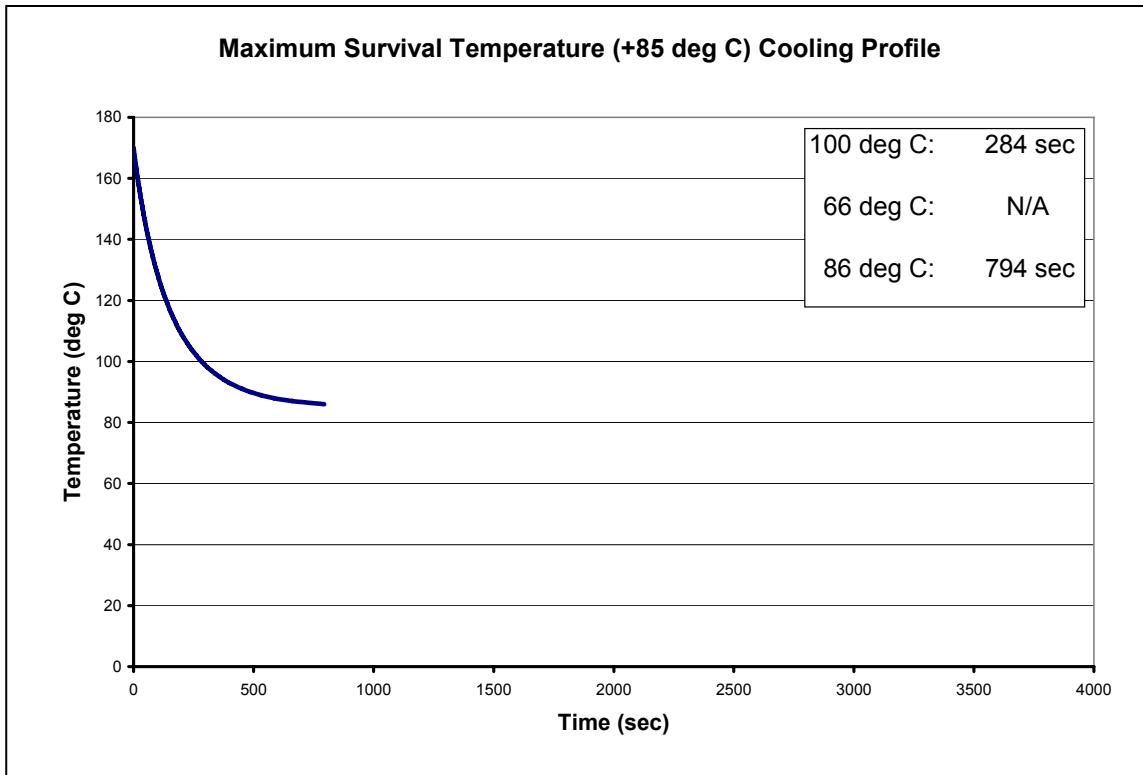


Figure 36: Calculated Sub-Tg Tube Cooling Profile, 85°C Ambient Temperature

The temperatures used in Figures 32, 33, 35 and 36 were chosen based on the survival (–60 to +85°C) and operating (–40 to +55°C) temperature ranges given for the Shuttle cargo bay (4). The ambient temperature used in Figure 34 was used to compare the calculated results with the experimental results, which has an ambient temperature of 30°C and an initial temperature of 166°C. The results are summed up in Table 10 below.

Table 10: Time to Event Temperatures

		Ambient Temp (°C)				
		- 60	- 40	30	55	85
Time to Temp (sec)	Vent Tube (100°C)	99	103	129	169	284
	Activate Actuators (66°C)	186	196	284	485	N/A
	Ambient	3964	3057	996	1075	794

As shown in the table above, the smaller the differential between the ambient and initial temperatures, the shorter the cooling time to 1°C above that ambient temperature. Times were calculated 1°C above ambient because the actual temperature approaches as a limit; it would take an infinite amount of time for the temperatures to match precisely.

The discrepancy in the time-to-temperature cooling profile for the 30°C ambient condition is due to the lower initial temperature, 166°C, used in the calculations. For the 85°C ambient condition, the tube will never reach the 66°C necessary for piezoelectric actuator activation.

The results from equation 12 will be checked against actual experimental results for validation. This will be shown in Chapter IV, Analysis and Results.

Thermal Test Setup and Procedures

For the first test on a sub-T_g tube, two Omega® CO1 “Cement-On” type-K thermocouples (operating range: –200 to 1250°C) (19) were attached to the exterior of the tube on the surface of the Kapton sheath. Unfortunately, when the tube deployed, the hotter of the thermocouples fell off. This was due to either the lack of adhesion to the slick, non-porous surface of the plastic, or the fact that the hotter thermocouple was heated beyond the maximum working temperature of the adhesive. Either way, it was determined that the external temperature measurements were not an ideal way of accurately measuring the cooling profile. The graphite/epoxy/thermoset plastic layer of the tube is of primary importance, considering it is the actual material that undergoes rigidization.

To measure the graphite/epoxy layer, the thermocouples were slid under the Kapton sheath (in the areas determined in the *Thermal Tests* section) and glued on using Permatex[®] Form-A-Gasket[®] No. 1 Sealant, which has a much higher maximum operating temperature than the original adhesive, 204.4°C (20).

The Thermofoil[™] resistive heaters were function-checked before the heater box was attached to the quarter-structure. These heaters have been used for testing for several years. This was done to verify they could still heat the tubes beyond glass-transition temperature. All tests were run using 24 volts and 3.50 amps to run the heaters. This is representative of the power the Shuttle will supply. The heaters easily met their performance criteria, heating one tube past 170°C, which is well beyond what is required for softening the tube.

The tests were run using a worksheet to track events. An example is shown below in Figure 37. Key parameters were monitored to validate that the tests were running properly. Times were monitored to signal when to initiate certain events and also served as a check to match up with the data being recorded electronically. The overall vacuum chamber pressure was monitored to ensure it was holding relatively steady. The pressure in the storage section was also observed closely to assure it was not leaking inflation air.

Step Description	Action	Time	Vacuum Chamber Pressure	Vessel Pressure
Start LabVIEW	Start	0		
Vacuum	Start	10	14.51	14.56
	Stop	1100	0.25	14.50
Heaters	Start	1150	0.25	
Thermocouples @ 125 deg C	Thermo #1	3347	0.27	14.54
	Thermo #2	2601	0.27	14.52
Thermo #1 above 125 for 600 sec (10 min)	Ready	3947	0.27	14.57
1. Camera	ON			
2. Heaters	OFF			
3. Latch	FIRE	3959		
4. Solenoid	FIRE			
Pressure Drop?		Slight		
Temperatures				
Thermo #1 @ 120 deg C		4004		
Thermo #2 @ 120 deg C	Vent Gas	4034	0.28	
Thermo #1 @ 90 deg C		4091		
Thermo #2 @ 90 deg C		4116		
Thermo #1 @ 60 deg C		4269		
Thermo #2 @ 60 deg C		4279		
Thermo #1 @ 30 deg C		6441		
Thermo #2 @ 30 deg C		7134		
Stop LabVIEW	Stop	7200		
Final Vacuum Chamber Pressure			0.29	
Vent Vacuum Chamber				

Figure 37: Example Spreadsheet Used for Tracking Tests

Chapter Summary

This chapter covered the background data necessary to run the required pressure and thermal tests. Also, the analytical predictions were calculated to compare with the experimental results. The primary equipment involved in testing was discussed to give the reader a better understanding of their function and operation. Finally, the timeline for testing was introduced in the form of the aforementioned spreadsheet.

IV. Analysis and Results

Chapter Overview

This chapter discusses the experimental results of the pressure and thermal tests and compares these results to their calculated values derived in the previous chapter, to check how well the data correlates.

Inflation Tests

The total system pressure measured agreed with the calculations performed in the design stage (Chapter III). The Mathcad[®] worksheet, which was created to calculate the pressure vessel size (Appendix A), predicted a system equalization pressure of 7.08 psia for the sub-Tg tube, assuming the gas temperature in the pressure vessel had equalized with the surrounding temperature of the vacuum chamber at 24.4°C. The vacuum chambers ambient air temperature varied from test to test due to slight changes in the room temperature. The initial equalized total system pressure for the two successful tests was 7.15 psia. This represents a discrepancy of about 1%.

The cloth tube test resulted in the same initial equalized pressure as the sub-Tg tube test, assuming the gas was at ‘room’ temperature, 23°C. The calculated value was 7.05 psia and the experimentally measured value was 7.17 psia. This represents a discrepancy of only 1.7%. The results are summarized in Table 11.

Table 11: Analytic vs. Experimental Pressurization Results

	Analytic (psia)	Experimental (psia)	Percent Difference
Sub-Tg Tube	7.08	7.15	0.99%
Cloth Tube	7.05	7.17	1.70%

There was a slight pressure leak measured before the tubes were vented, this is why the initial equalized pressures were used as opposed to an average. The leak was most likely due to the flexible connection between the stainless steel and plastic tubing (Figure 38). Too much or too little force on this connection could pry open a slight gap.

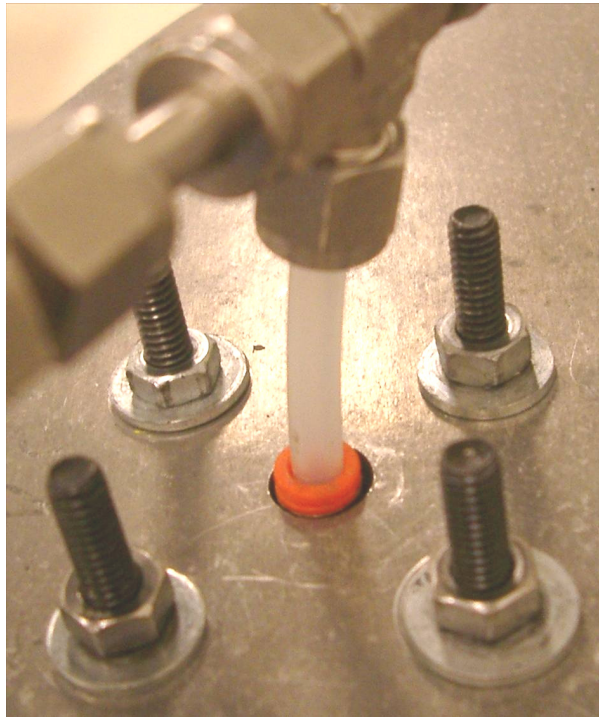


Figure 38: Plastic Tubing Connection

Even with this slight pressure loss, the tube retained pressure above 4 psia long enough to assure the tube fully deployed, cooled and rigidized. For the test below, the hottest temperature on the tube was monitored down to 100°C before the gas was vented to ensure rigidization. Figures 39 and 40 display graphically the results obtained from the sub-Tg and cloth tube tests, respectively.

The *Overall Analysis and Results* section at the end of this chapter discusses both the pressure and thermal tests together.

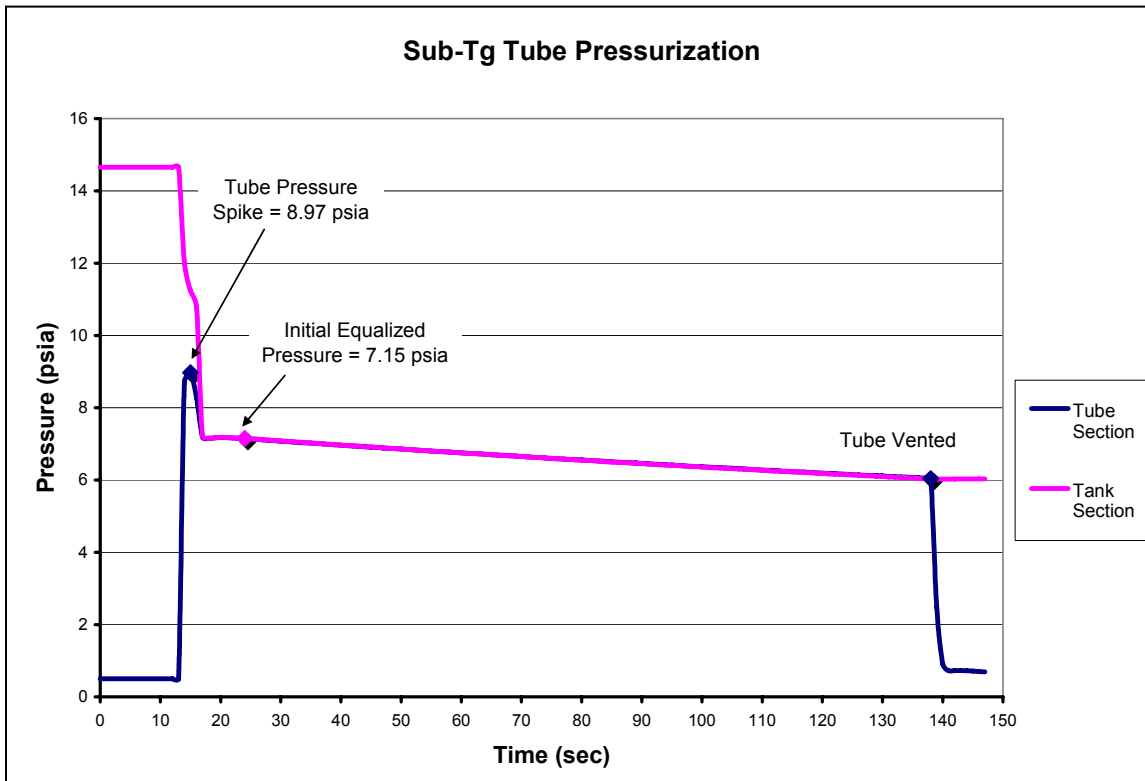


Figure 39: Sub-Tg Tube Pressurization

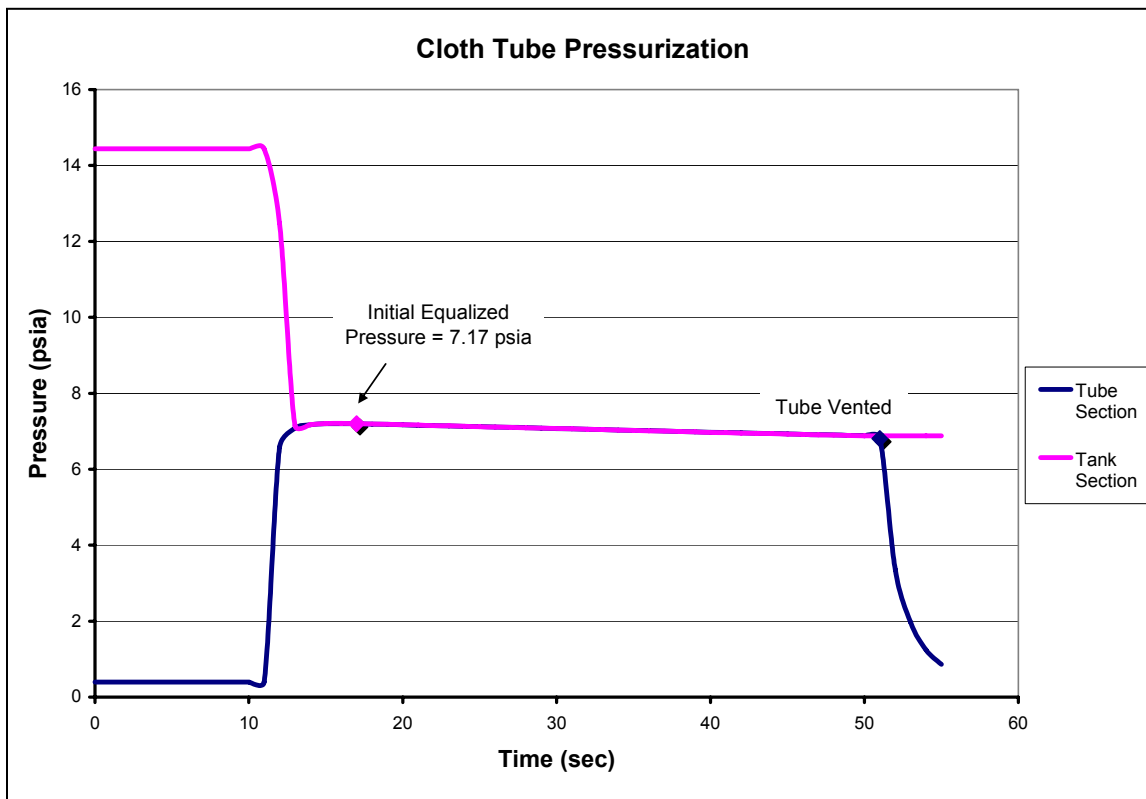


Figure 40: Cloth Tube Pressurization

The pressure spike in the sub-Tg pressure profile was inadvertently caused by user error. Both the solenoid, which separates the two sections of the pressure system, and latch, which holds the tube in place before deployment, were meant to be opened at the same instant. Instead, the solenoid was opened two seconds before the latch. This caused the tube to be pressurized before its full volume was available to the incoming gas. Fortunately this action did not cause tube failure due to overpressure. The pressure spiked only to about 9 psia, below the 10 psia maximum.

Aside from user error, there were quite a few problems encountered with the sub-Tg tube pressure tests. Most notable were leaks in several parts of the system, causing

the tubes to lose pressure so quickly they would not inflate fully (Figure 41). Two tubes that were re-folded to their original state contained breeches at the fold points. One of the tubes was also breeched between the sub-Tg material and the aluminum end cap. These leaks could have been caused by the tubes being folded and/or flexed before they reached their transition temperature, or possibly from overpressure during previous testing done with the 400 psi pressure system.

Other pressure leaks occurred due to improper o-ring fittings and a large crack in the base of the heater box, which was inadvertently caused by over-tightening the hold-down bolts. This issue was fixed in the current design by removing the small plastic standoffs from the base of the heater box. The standoffs were originally designed to fit a layer of fiberglass insulation beneath the heater box, however, the insulation on the base was deemed unnecessary and therefore removed along with the standoffs.



Figure 41: Tubes not Fully Inflated

Due to the fact that the modified system pressure was zero psig and leaks could not be discovered while the structure was in the vacuum tank, they were located using a large nitrogen pressure tank hooked up at the fill point of the system. However, there were no leakage problems with the modified system hardware. The new tubing and component connections held pressure throughout every test performed.

Tubes were refolded using a large oven. After two refolded tubes were found to have pressure breeches, the latter tubes were heated past transition temperature to 150°C and stabilized there for 10 – 15 minutes. This was done to assure the refolding process would not cause any fiber breakage or tearing in the Kapton. The earlier tubes were probably damaged due to improper folding and heating. The final tube tested held pressure after being refolded, attesting to the fact that the tubes are reusable, as specified by L'Garde (8).

Thermal Tests

After the several failed pressurization tests due to leaks in the system, one tube was finally deployed. Only the one successful full heating and cooling profile test was run due to time constraints. However, the heating profiles of tubes before deployment were relatively consistent over several tests, using the thermocouple location #1. The slight differences seen in Table 12 can be attributed mainly to the refolded tubes, rather than slight differences in initial temperatures.

Table 12: Tube Heating Times

Test	Temperature in Vacuum Chamber (°C)	Time to 125°C (minutes)
1	22.3	34.4
2	23.1	36.8
3	22.2	36.9
4	23.0	36.9
5	22.9	36.4

After the initial test, the refolded tubes did not fit flush in the heater box. The end-cap would rest on the top of the box rather than in the recessed portion. The results from the successful thermal test are shown below in Figure 42.

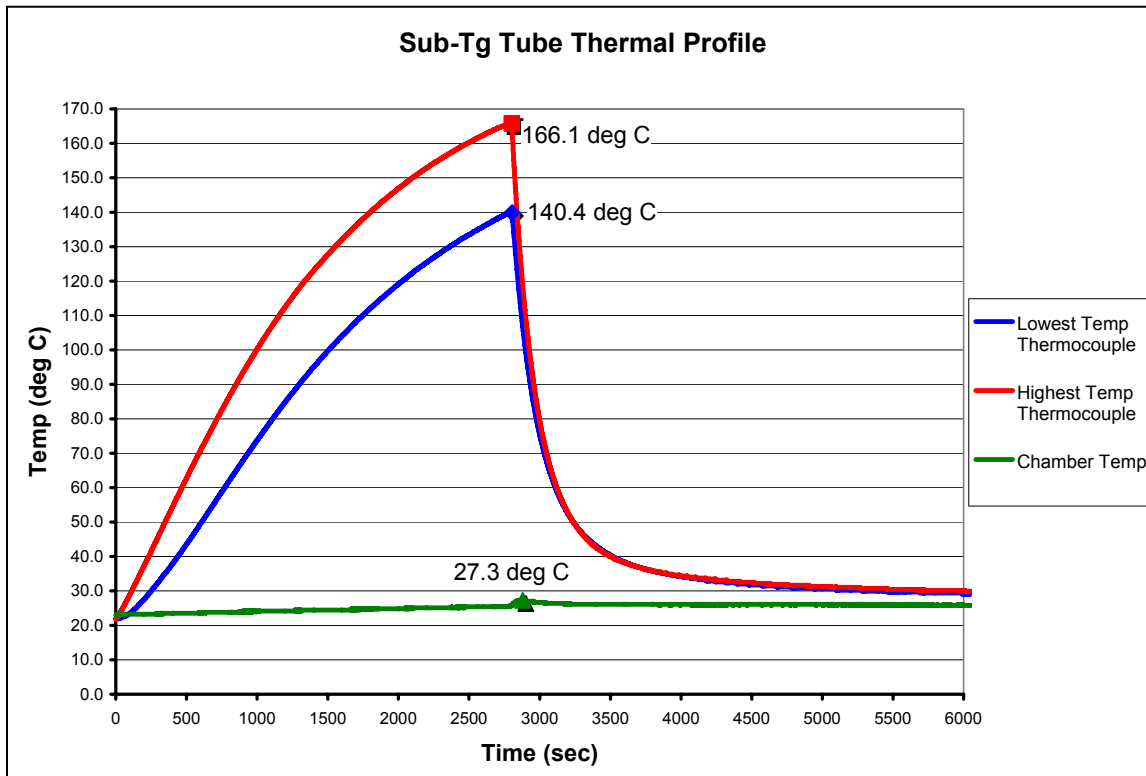


Figure 42: Sub-Tg Tube Thermal Profile

This chart shows the entire thermal profile of the sub-Tg tube. There was a 600 second (10 minute) delay before deployment added after the cooler thermocouple reached 125°C. This was done for every test performed. Even though the entire tube had crossed the glass-transition threshold, the pause was added because it is unknown whether the tube is instantly soft enough once it hits 125°C, or whether the material needs time to equalize before becoming fully flexible. The 600 second delay should be used in flight as a factor of safety, especially now that the power demands are more relaxed.

Figure 43 displays the cooling profile only.

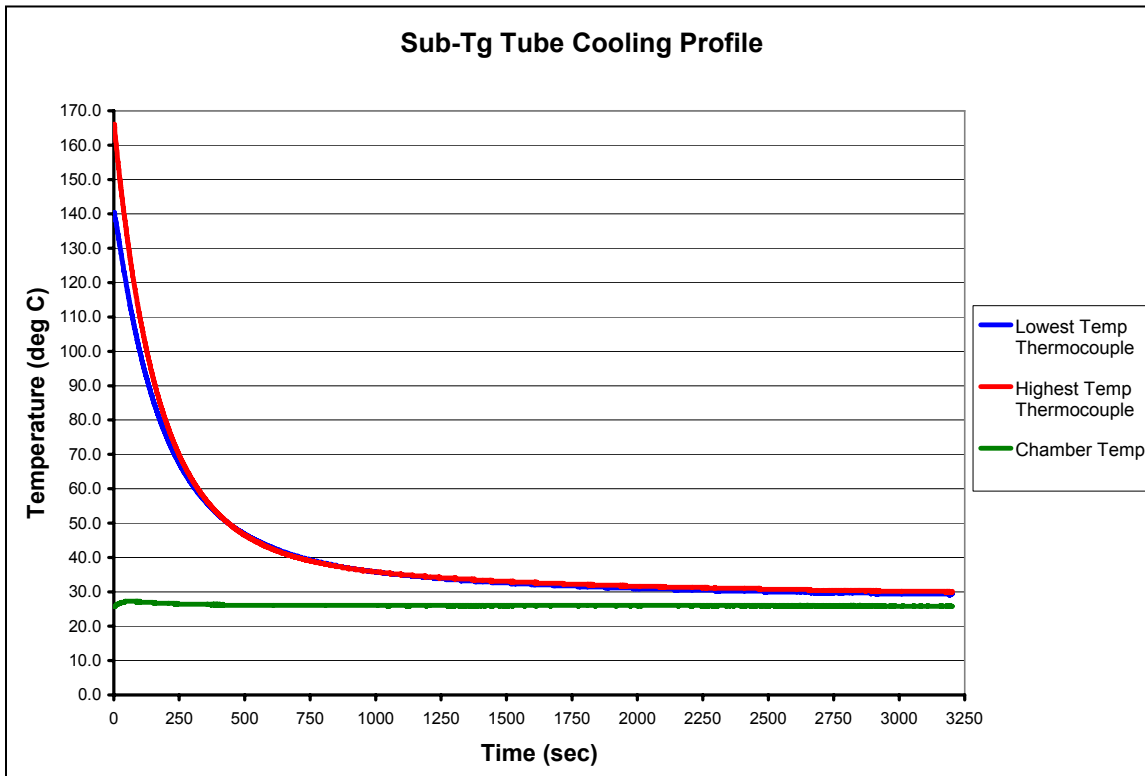


Figure 43: Sub-Tg Tube Cooling Profile

From this chart, it can be seen that once deployed, the tube cools off relatively quickly initially, and slowly approaches the ambient vacuum chamber temperature as a limit. The highest temperature thermocouple reached 166.1°C and still dropped to the 100°C venting temperature in only 125 seconds.

As stated in Chapter III, the cooling profile was needed to verify times for certain operational events. The graphs in Figures 44 and 45 below compare the experimental to the predicted results.

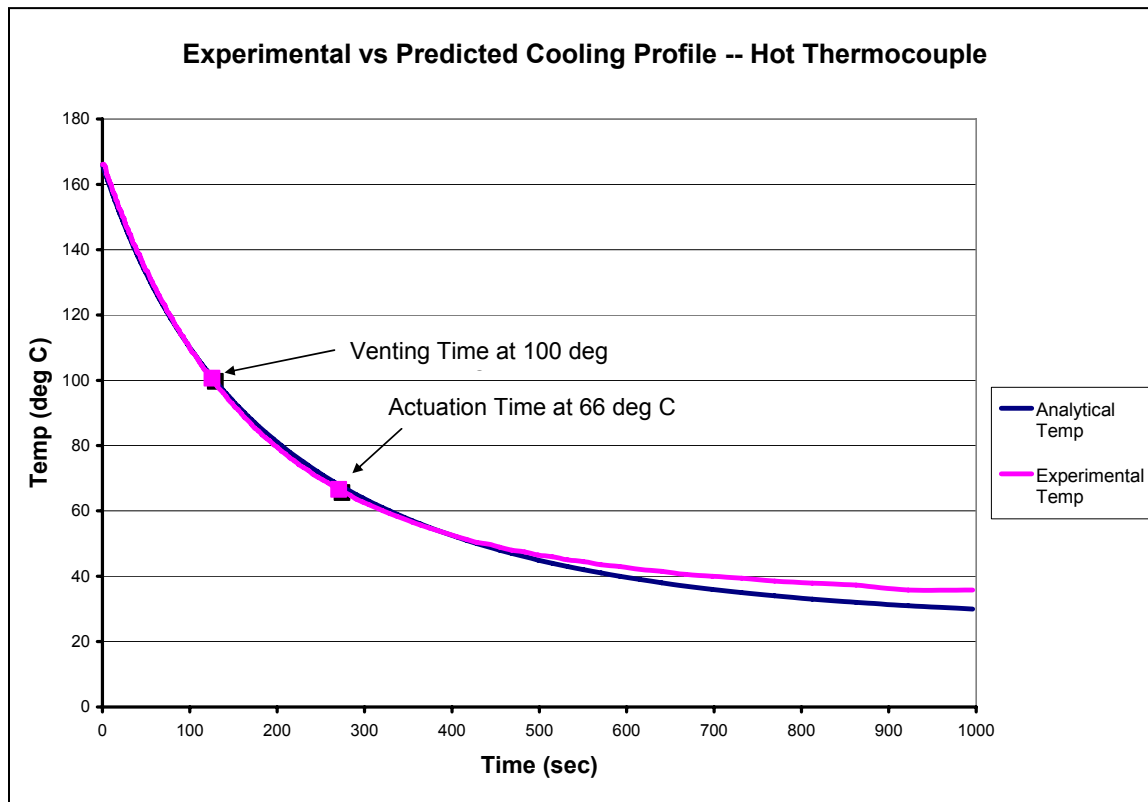


Figure 44: Experimental vs. Analytical Cooling Profile – Hot Thermocouple

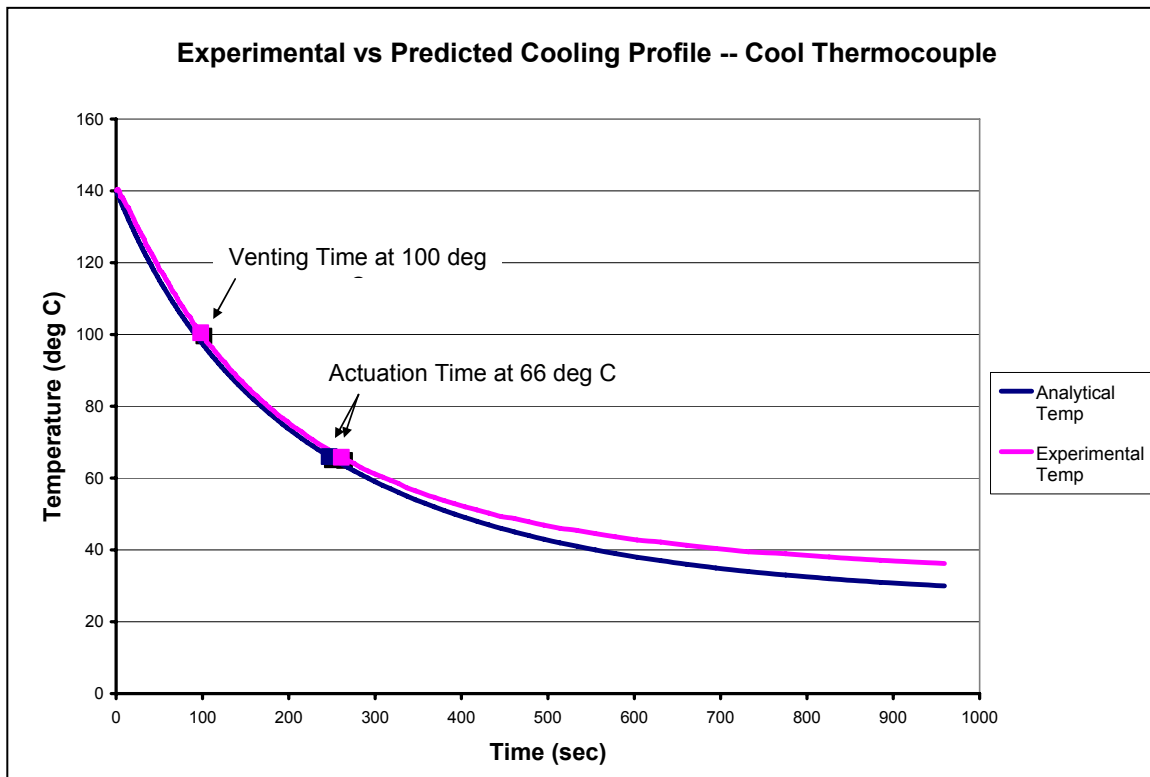


Figure 45: Experimental vs. Analytical Cooling Profile – Cool Thermocouple

The slight discrepancies between the experimental vs. predicted temperatures at lower temperatures are attributed to heat transfer by conduction. As the delta between the tube temperature and the ambient temperature decreased, heat transfer by radiation contributed less and heat transfer by conduction took over. The predicted values follow a radiation-only cooling profile which predicts a quicker cooling time than actual. However, since the tube material has relatively small thermal conductivity, it holds the heat longer, extending the actual cooling time. A closer approximation to actual results could have been calculated by combining cooling by radiation *and conduction* in the lumped capacitance method shown in Chapter III. This was not deemed necessary,

however, due to the fact that all key events for the experiment occur far above the range where conduction plays a significant role. Table 13 displays the temperatures of the two key events for the hottest thermocouple and the time it took experimentally to reach each event. Since the hottest point on the tube was measured down to these temperatures, the rest of the tube would fall below these maximum values.

Table 13: Predicted vs. Experimental Key Events

Event	Event Temperature (°C)	Experimental Time (sec)	Predicted Time (sec)	Percent Difference
Vent Gas	100	125	129	3.2%
Piezoelectric Patch Actuation	66	274	284	3.7%

During the several run-ups of the heater boxes, an interesting trend was observed. There was up to a 30°C difference in temperature between the coolest and hottest part of the tube. This difference stayed constant once the tube reached a steady-state heating condition while the heater box was still running. Adding 30°C to the temperature read by the thermocouple on the slowest-heating portion of the tube will accurately predict the maximum temperature on the tube. This observation was used in Chapter III to determine the predicted tube cooling profiles. The large gradient illustrates the significance of knowing the thermal profile along the entire length of the tubes.

Overall Analysis and Results

The previous sections analyzed results from the pressurization and thermal tests separately. This section analyzes the results together and discusses their significance.

The graph shown in Figure 46 displays both pressure and thermal results on the same time scale. The left-side y-axis shows the temperature of the tube in °C, while the right-side y-axis displays the corresponding tube pressure in psia.

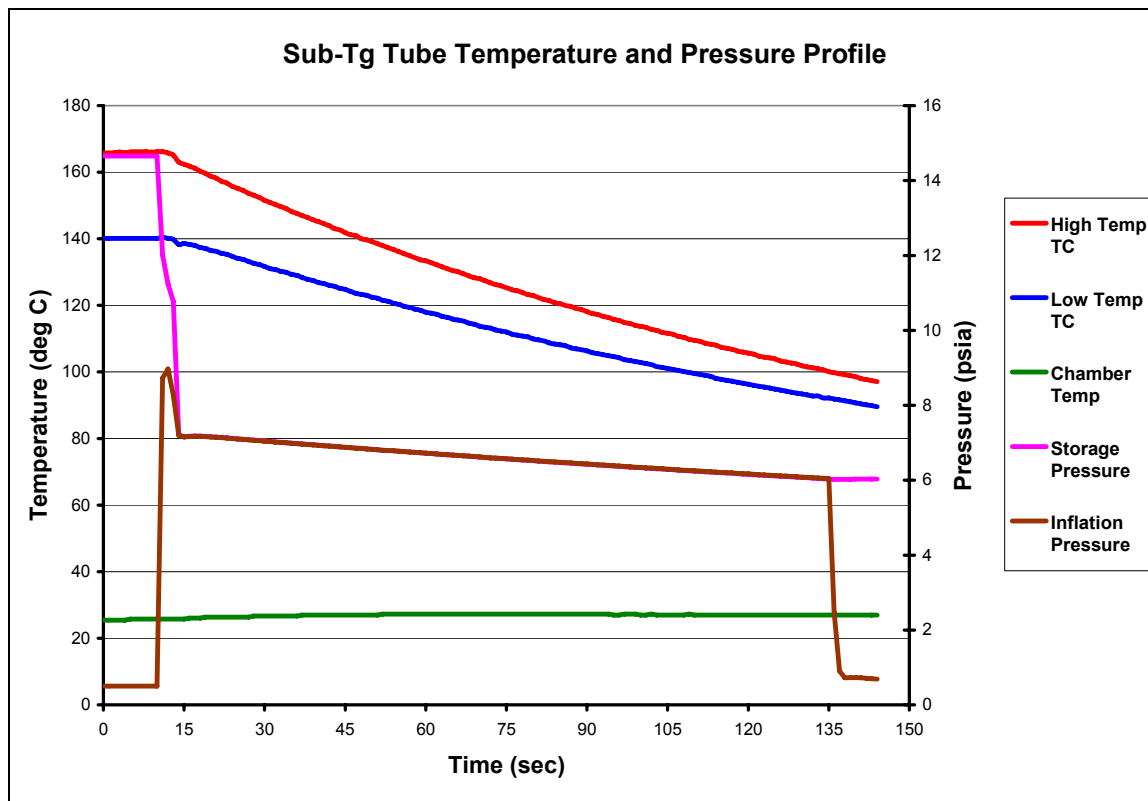


Figure 46: Sub-Tg Pressure and Thermal Profile during Deployment

From the graph it is evident that the entire tube, evaluated at its hottest point, cooled down from 166°C to 100°C in about two minutes (125 seconds). The tube was vented at this point, leaving the rigidized tube to continue its cooling without the inflation air inside. From this point on, as conveyed in the *Thermal Tests* section above, the tube cooled to the maximum operating temperature of the piezoelectric actuators (66°C) in less than five minutes (274 seconds).

Chapter Summary

This chapter covered the analysis and results from the tests run. The pressure calculations correlated very closely with the predicted values, coming in with under a 2% difference. This minute discrepancy could possibly be attributed to either a slight miscalculation in system volume and/or gas temperature at deployment.

The thermal tests revealed that the cooling profiles could be determined accurately for a given ambient temperature, coming in with under a 4% difference for critical experiment event times.

Overall, these results illustrate that experimental results can be accurately predicted with calculations. This strengthens the fundamental understanding of the RIGEX systems discussed, and increases confidence of experiment success on orbit.

V. Conclusions and Recommendations

Chapter Overview

This chapter discusses the conclusions drawn from this thesis work and covers recommendations for future research and RIGEX modifications. The final pressure system design is compared to its predecessors and the significance of the thermal profile of the tubes is reiterated. Recommendations include structural and sensor modifications necessary to complete the pressurization system for flight, and necessary computer code modifications for the power and thermal systems.

Conclusions

As mentioned in Chapter II, the pressurization system has undergone many modifications since the original design. The below figures (Figures 47 – 50) graphically illustrate the evolution of the system from concept to current design.

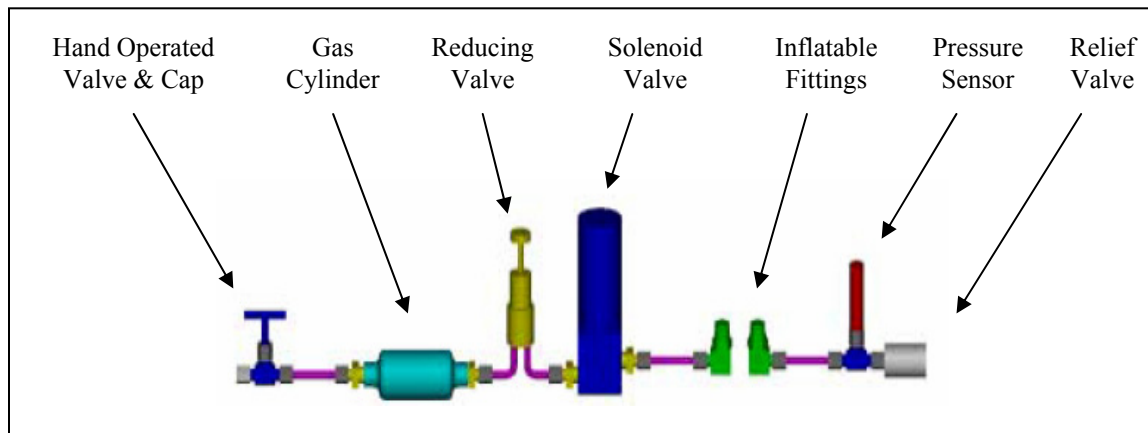


Figure 47: Initial Pressure System Concept (3)

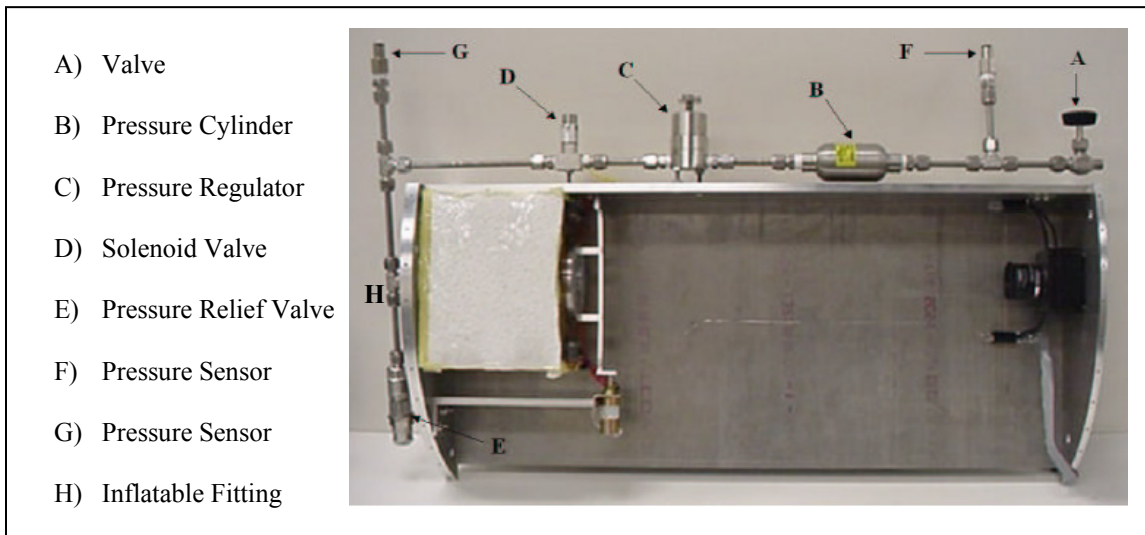


Figure 48: First Assembly of Pressure System (21)

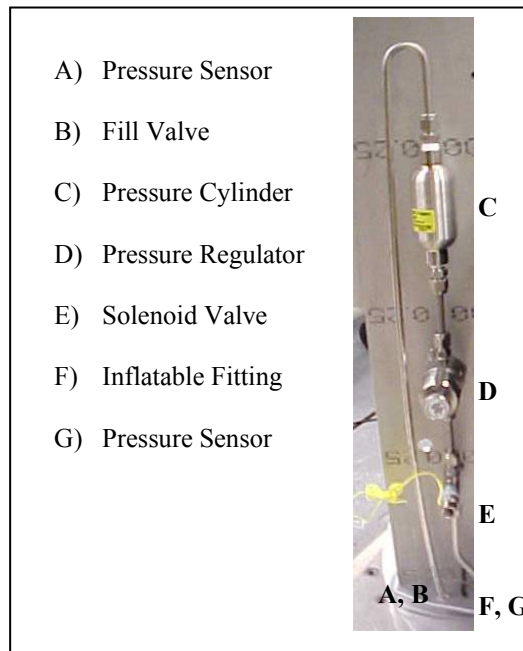


Figure 49: Second Assembly of Pressure System (14)

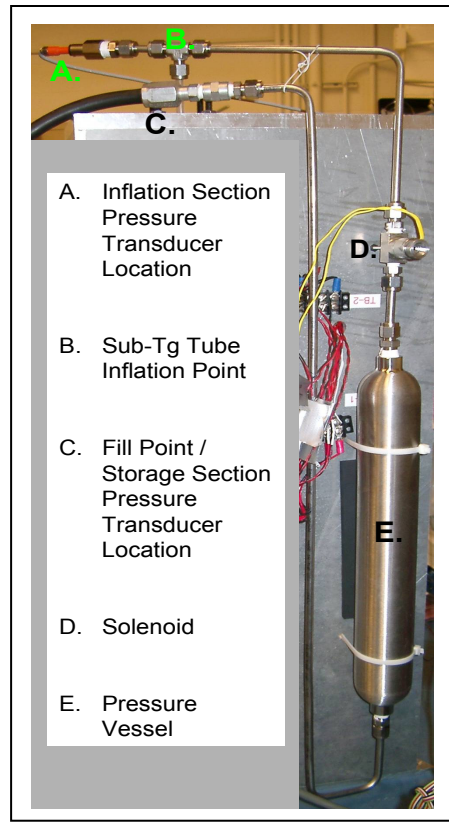


Figure 50: Final Design of Pressure System

The new pressure system has many advantages of the original design. The larger pressure vessels, fewer components, and fewer potential leak points all contribute to system reliability and safety and were discussed in detail in Chapter IV.

There is one significant disadvantage of the new pressure system inherent in its design. Should there be anything more than a slight pressure leak, there will be no back-up gas to compensate. Even if the larger tanks were pressurized beyond 14.7 psia to provide additional gas, there is no regulator to suppress the increased flow. The flow would almost certainly increase the tube pressure beyond its maximum limit and cause significant if not catastrophic failure of one or more RIGEX experiment bays.

As stated in Chapter IV, the full thermal analysis for RIGEX is extremely important to have. Almost all experiment objectives, with the exception of camera operation and data recording, directly depend on where a tube is at in its temperature profile. A full thermal analysis has now been recorded from heater start-up through deployment and back down to the ambient temperature.

Recommendations

Modifications to the RIGEX main structure are needed to incorporate the new pressure system. Two holes in three of the four sides of the battery-box cover are necessary to run tubing through. One is to run the tubing from the fill points to the pressure vessels, and the other leads to the base of the tube (inflation point) and the downstream pressure transducer. Also, some means of clamping down the tubing must be found to keep the longest free lengths from vibrating violently during launch. Loose tubing could resonate or simply be forced into failure by the g-forces involved. This issue should be resolved through vibration testing.

Other modifications to the main structure need to be included to fit RIGEX soundly into the CAPE canister. NASA has requested a metal sheath be fitted around the entire structure to keep CAPE's Teflon-coated interior from being damaged by loose components, end-caps, etc... (1). RIGEX's diameter is only 19.75" where as the CAPE interior diameter is 21.0". This leaves a gap of 5/8" around the RIGEX main structure. Bumpers were conceptualized and designed by Holstein (9). These bumpers have Viton[®] rubber facing and adjustable-length arms which can be constructed to fit snugly against

the CAPE interior. The other end of the RIGEX structure will be securely bolted to one of CAPE's end-caps.

Space-rated *absolute* (psia) pressure transducers are needed in the final assembly. The plastic sensors used in testing should be replaced with high-quality transducers that can be locked in place. These transducers should be ordered and installed so that they can be used in ground tests and so that their performance is well understood.

Measurement of the ambient temperature can be recorded by any thermocouple inside the RIGEX envelope before heating begins. This should be done to create a set-point for cooling profile calculations. Calculations should also use 170°C as the initial temperature. After the thermocouple in the slowest-heating tube fold reads 125°C (glass-transition temperature), the heaters should be programmed to stay on for an additional 600 seconds (10 minutes) to assure the tubes are soft enough for deployment.

Should the ambient temperature in the Shuttle cargo bay stay above 66°C during testing, the computer code should proceed to initiate the piezoelectric patches when the tubes reach 1°C above the ambient temperature. This is far from optimal, but results could likely be interpreted back on the ground with above-maximum-temperature testing on the piezoelectrics to characterize their performance at any high ambient temperature.

Modifications to the programming need to be accomplished. The lumped capacitance equation (Equation 12) needs to be incorporated to adapt timing for critical RIGEX events. The 600-second deployment delay mentioned above should be programmed in as well.

The electrical system will require some modification due to the conversion to Shuttle power. Some of the RIGEX components were to be wired directly to the battery packs. Also, the power distribution needs to be revisited. The standard power coming off of the Shuttle will be 24V and 3.5A. All components were not initially set-up to operate using these values. Along with these modifications, wiring harnesses need to be constructed from all subsystems to the PC-104 flight computer. The wiring used must meet NASA specifications.

The resistance of the ThermofoilTM heaters should be tested for each heater box before installation. Even when the heater patches are the same size, they were shown to have different resistance values. Their circuits should be wired so that they will reflect, as closely as possible, the total resistance values their original design specifies (21).

The parties interested in the results from RIGEX (28, 31) would specifically like detailed data on fiber-breakage of the sub-T_g tube material. In their current state, the tubes would likely be destroyed on reentry due to the fact they are cantilevered with a large mass on their free ends and the fact that the forced-vibration would shake them violently. So that the deployed tubes are not destroyed, some type of bracing would be required. This could possibly be accomplished with inflatable foam or a mechanical clamping system. This area needs further study if it is determined that the tubes should be preserved.

A full end-to-end three-tube experiment test needs to be accomplished to assure full operation and coordination of all components. To be the most accurate, the full experiment should be fully assembled, shaken on a shaker table to simulate launch,

mounted in a large vacuum chamber, powered up when the chamber is evacuated, allowed to run all three tests, then removed from the chamber and shaken again to simulate reentry. If all tubes deploy successfully and the recorded data comes back intact, then the experiment would justify its validity.

Summary

The primary goals of this thesis, as stated in Chapter I, were to improve upon the current RIGEX design by resolving critical issues encountered with the pressurization system, validate the cooling profile of the sub-Tg tubes, manage manifestation on the Space Shuttle through the Space Test Program (STP) and NASA, and incorporate any necessary changes to the experiment due to the introduction of a new payload envelope.

Throughout this endeavor, many essential changes to RIGEX were incorporated into an already well configured design. The upgraded pressure system and cooling profile will increase RIGEX success on-orbit. Briefings were presented to the Air Force and DoD SERBs to improve the chances of a Shuttle flight. Modifications allowed by the change from the GAS canister to CAPE assisted in many RIGEX system upgrades. The current status of RIGEX is shown in Table 14, as compared to Table 5 in Chapter II. Two components have been added from the above *Recommendations* section, the ‘wiring layout/harness’ and the ‘tube bracing for reentry.’

Table 14: Status of RIGEX after Current Thesis Work

Component	Initial Design	Prototyped	Tested	Finalized
Heater Box	✓	✓	✓	✓
Pin-Puller/Latch	✓	✓	✓	✓
Image System	✓	✓	✓	✓
PC-104 Computer	✓	✓		
Inflation System	✓	✓	✓	✓
Piezoelectric Actuators	✓	✓	✓	✓
Accelerometers	✓	✓	✓	✓
Wiring Layout/Harnesses				
Tube Bracing for Reentry				
Main Structure	✓			

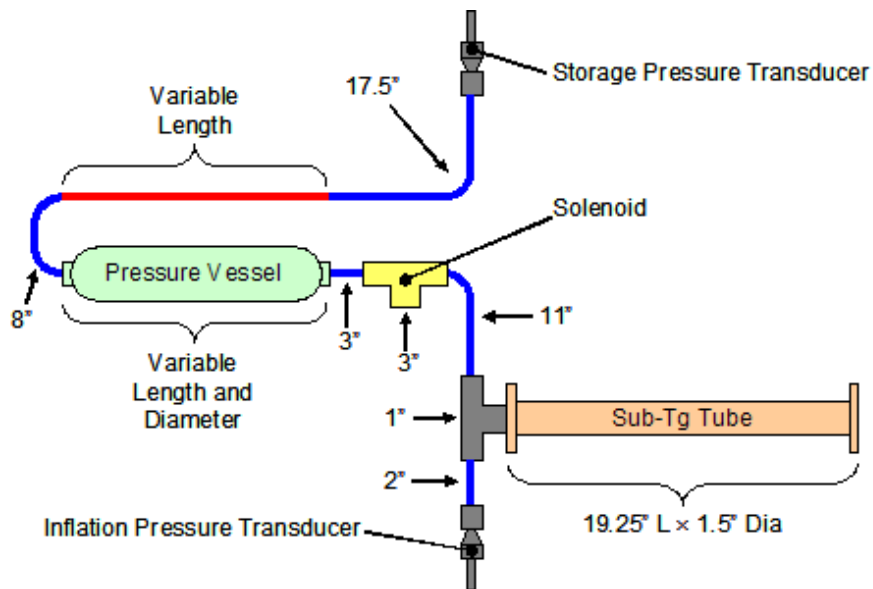
RIGEX is close to completion. Many students and advisors have poured their efforts into completion of this experiment. The data gained by RIGEX will be a stepping stone to understanding the behavior of inflatable/rigidizables in space and validating their use. Not only would the successful launch, implementation and recovery of RIGEX be beneficial to those involved in its construction, AFIT, and the space community, but it would revolutionize the use of extremely large space structures for future endeavors.

Appendix A: Mathcad® Pressure Vessel Calculation Worksheet

Use Universal Gas Law to Calculate the # of Moles of Air/N₂:

$$P \cdot V = n \cdot R \cdot T \quad \Rightarrow \quad n = \frac{P \cdot V}{R \cdot T}$$

The number of moles in the storage section will equal the number of moles in the entire system once the solenoid is open (conservation of mass).



The **red** tubing changes length based on pressure vessel length, the **blue** does not.

Volume of a Cylinder (for tubing, joint and transducer calculations):

$$V_{\text{cyl}} = \pi \cdot r^2 \cdot h \quad \text{where } h \text{ is the length of the pipe and } r \text{ is the inner diameter}$$

Pressure Vessel Variables:

$$V_{\text{Vessel}} := 500 \text{ cm}^3$$

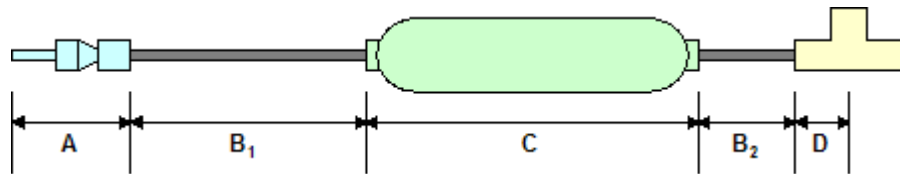
$$L_{\text{Vessel}} := 13.8 \text{ in}$$

Change these two dependent variables based on Pressure Vessel chosen...

$$\Delta_{\text{tube}} := L_{\text{Vessel}}$$

$$\Rightarrow \Delta_{\text{tube}} = 13.8 \text{ in}$$

Sum-Up Volume of Storage & Inflation Sections:



$$V_A := \pi \cdot \left(\frac{3}{32} \text{ in} \right)^2 \cdot 1 \text{ in} \quad \Rightarrow \quad V_A = \blacksquare \text{ in}^3$$

$$V_B = V_{B1} + V_{B2} \quad V_{B1} := \pi \cdot \left(\frac{3}{32} \cdot \text{in} \right)^2 \cdot (17.5 \text{ in} + \Delta_{\text{tube}} + 8 \text{ in})$$

$$V_{B2} := \pi \cdot \left(\frac{3}{32} \cdot \text{in} \right)^2 \cdot 3 \text{ in}$$

$$\Rightarrow \quad V_B := V_{B1} + V_{B2} \quad \Rightarrow \quad V_B = \blacksquare \text{ in}^3$$

$$V_C := V_{\text{Vessel}} \quad \Rightarrow \quad V_C = \blacksquare \text{ in}^3$$

$$V_D := \left(\frac{1}{2} \right) \cdot \pi \cdot \left(\frac{3}{32} \text{ in} \right)^2 \cdot 3 \text{ in} \quad \Rightarrow \quad V_D = \blacksquare \text{ in}^3$$

$$V_{\text{Storage}} := V_A + V_B + V_C + V_D \quad \therefore \quad V_{\text{Storage}} = \blacksquare \text{ L}$$

$$V_F := V_D \quad \Rightarrow \quad V_F = \blacksquare \text{ in}^3$$

$$V_G = V_{G1} + V_{G2}$$

$$\Rightarrow \quad V_G := \pi \cdot \left(\frac{3}{32} \text{ in} \right)^2 \cdot (11 \text{ in} + 2 \text{ in})$$

$$\Rightarrow \quad V_G = \blacksquare \text{ in}^3$$

$$V_H := \pi \cdot \left(\frac{3}{32} \text{ in} \right)^2 \cdot 1 \text{ in} \quad \Rightarrow \quad V_H = \blacksquare \text{ in}^3$$

$$V_I := V_A \quad \Rightarrow \quad V_I = \blacksquare \text{ in}^3$$

$$V_J := \pi \cdot \left(\frac{3}{4} \text{ in} \right)^2 \cdot 19.25 \text{ in} \quad \Rightarrow \quad V_J = \blacksquare \text{ in}^3$$

$$V_{\text{Inflation}} := V_F + V_G + V_H + V_I + V_J$$

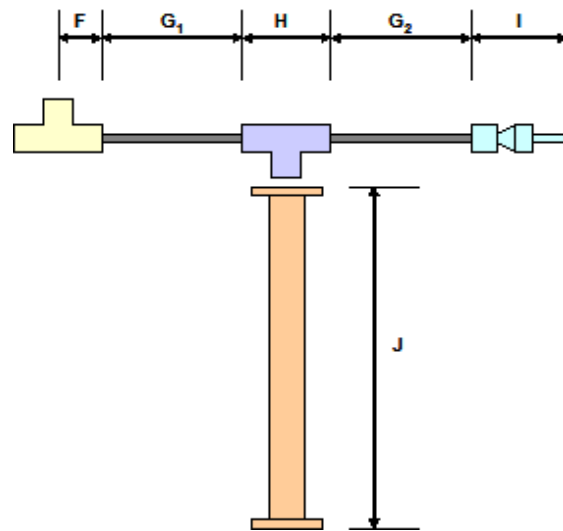
∴

$$V_{\text{Inflation}} = \blacksquare \text{ L}$$

$$V_{\text{Entire_Sys}} := V_{\text{Storage}} + V_{\text{Inflation}}$$

∴

$$V_{\text{Entire_Sys}} = \blacksquare \text{ L}$$



Using Standard Temp & Pressure (STP):

$$P_{\text{Storage}} := 760 \text{ torr} \quad (\text{Atmospheric Pressure})$$

$$R := 62.36 \frac{\text{L} \cdot \text{torr}}{\text{mol} \cdot \text{K}} \quad (\text{Gas Constant})$$

$$T_{\text{Ground}} := 300 \text{ K} \quad (\text{'Room' Temperature, check } P_{\text{Final}} \text{ with upper \& lower temps in LEO:})$$

Minimum & Maximum Temperatures in LEO: (Survival Temp Range* is -60°C to +85°C)

$$T_{\text{LEO_min}} := 273.15 \text{ K} - 60 \text{ K} \Rightarrow T_{\text{LEO_min}} = \blacksquare$$

* From CAPE Hardware
Users Guide

$$T_{\text{LEO_max}} := 273.15 \text{ K} + 85 \text{ K} \Rightarrow T_{\text{LEO_max}} = \blacksquare$$

Moles of Air/N₂ in Storage Section:

$$n := \frac{P_{\text{Storage}} \cdot V_{\text{Storage}}}{R \cdot T_{\text{Ground}}}$$

Pressure of Entire System at Equilibrium (must be between 4 psi & 10 psi!):

$$\text{For: } V_{\text{Vessel}} = \text{cm}^3$$

Proof of Combined Gas Law:

$$P_{\text{Final}} = \frac{n \cdot R \cdot T}{V_{\text{Entire_Sys}}} = \frac{\left(\frac{P_{\text{Storage}} \cdot V_{\text{Storage}}}{R \cdot T_{\text{Ground}}} \right) \cdot R \cdot T_{\text{LEO}}}{V_{\text{Entire_Sys}}} = \frac{P_{\text{Storage}} \cdot V_{\text{Storage}} \cdot T_{\text{LEO}}}{V_{\text{Entire_Sys}} \cdot T_{\text{Ground}}}$$

$$P_{\text{Final_Min}} := \frac{P_{\text{Storage}} \cdot V_{\text{Storage}} \cdot T_{\text{LEO_min}}}{V_{\text{Entire_Sys}} \cdot T_{\text{Ground}}} \Rightarrow P_{\text{Final_Min}} = \blacksquare \text{ psi}$$

$$P_{\text{Final_Max}} := \frac{P_{\text{Storage}} \cdot V_{\text{Storage}} \cdot T_{\text{LEO_max}}}{V_{\text{Entire_Sys}} \cdot T_{\text{Ground}}} \Rightarrow P_{\text{Final_Max}} = \blacksquare \text{ psi}$$

Pressure Needs to be Between 4 psi (min. inflation pressure) & 10 psi (max. allowable tube pressure).

Appendix B: LabVIEW Program and Test Equipment Overview

National Instruments (NI) LabVIEW program was used for all data acquisition during vacuum chamber testing.

A customized LabVIEW program was created to monitor:

1. pressure in the storage section,
2. pressure in the inflation section (containing the sub-Tg tube),
3. temperature of the coolest area on the tube,
4. temperature of the hottest area on the tube, and
5. ambient temperature in the vacuum chamber.

The pressure data was recorded from the pressure transducers into Endevco pressure meters (Figure 51). This data was converted into voltage because the version of LabVIEW used could not read pressure directly. The voltage readings were then fed into a NI SCXI 1321 module attached to a NI SCXI-1000 docking station (Figure 52), which in turn fed the data into the LabVIEW computer. The voltages were recorded and converted to absolute pressure values in Excel.



Figure 51: NI Modules/Docking Station



Figure 52: Endevco Pressure Meters

The temperature values were recorded by LabVIEW in Fahrenheit. The thermocouples were attached to a NI SCXI 1112 thermocouple amplifier which was also attached to the NI docking station. The values were fed into the LabVIEW computer and were also converted in Excel to produce Celsius readings.

Power was supplied to the various subsystems individually. The Thermofoil™ heaters were powered by an Agilent 6038A System Power Supply (Figure 53). The lights, pin-puller, and solenoid valve were all powered separately by three Hewlett-Packard 6205B Dual DC Power Supplies (Figure 54).



Figure 53: Agilent System Power Supply

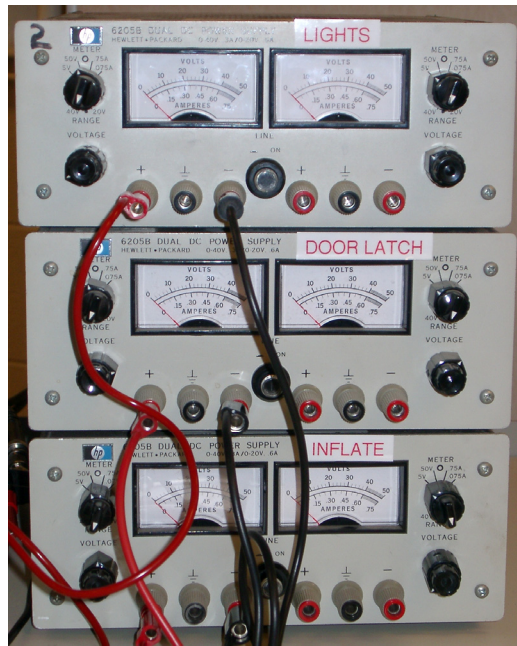





Figure 54: Hewlett-Packard Dual DC Power Supplies

Appendix C: 2004 DoD SERB Briefing Slides




Rigidizable Inflatable Get-Away-Special Experiment (RIGEX) AFIT-0301

DoD Space Experiments
Review Board
15 - 17 Nov 2004


Capt Chad R. Moeller
chad.moeller@afit.edu

Air Force Institute of
Technology

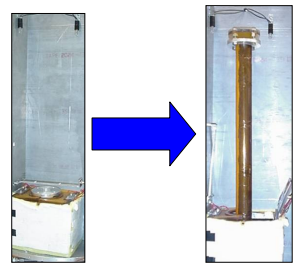
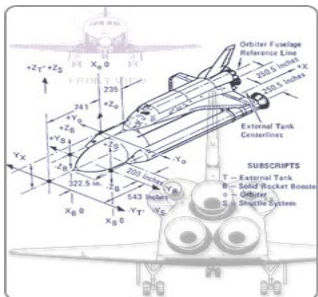
PI, Dr. Rich Cobb
richard.cobb@afit.edu



Concept



- **Objective:** Produce and fly experiment to collect data on inflatable rigidized structures in the space environment
- **Concept:**
 - Launch on Shuttle in self-contained *Container for All Payload Ejections* (CAPE) canister
 - Heat and inflate individual tubes
 - Cool tubes to make them structurally stiff
 - Vibrate stiffened tubes using piezoelectric patches
 - Collect data on inflation and vibration with environmental, video, and vibration sensors
 - Analyze tubes on return to determine effects of deployment on composite material



Concept

Continued



Comparison to Mechanical Structure



24-foot long truss, sub-Tg composite,
weight: 9 lbs

RIGEX Tube Properties

Property Description	Value	Units
Tube Diameter	1.5	inches
Tube Material Thickness	15	mils
Young's Modulus	$9.5E \times 10^6$	lbf/in ²
Moment of Inertia	19.881×10^{-3}	in ⁴
Material Density	53.957	lbf/ft ³

- **Advantages over Comparable Mechanical Systems:**

- Launch Cost Savings:
 - Weight Savings
 - Volume Savings
- Engineering Cost Savings
- Production Cost Savings

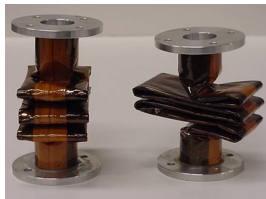
= **Substantial \$\$\$\$\$ Saved**



Key Components



- Inflatable Tubes
 - Graphite/epoxy
 - Thermoset plastic
 - 125°C glass-transition temperature
 - Excited with piezoelectric patch for characterization



Folded Tubes



Inflated/Rigidized
Tube

- Piezoelectric Patch:
Macro Fiber Composite (MFC)
 - First Flight – will test performance in space
 - Developed by NASA-Langley
 - Enabling technology for smart-structures

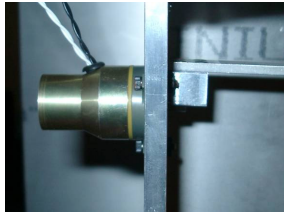


Piezoelectric Patch



Key Components

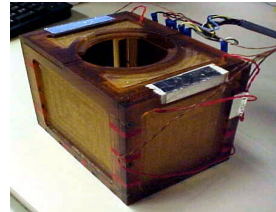
Continued



Shape Memory Pin-Puller



Pressurization System



Flight Oven



Flight Computer



Tri-Axial Accelerometer



RIGEX Structure



Justification



Military Relevancy (900km) Visible Spectrum

- Specific AF Prioritized Needs (collection resolution improved by larger apertures)
 - Any need that relies on remote monitoring and collection
 - Mid Term:
#6, 7, 16, 17, 22, 23 – Collect on and monitor various events
 - Far Term:
#20, 21, 22, 23, 29, 30 – Collect on and monitor various events
- RIGEX data is a step toward making inflatable space structures more viable
 - Large aperture sensors, large space structures, solar sails, solar power collectors, space telescopes, etc.
- Efforts currently supported by NRO and JPL
 - Letters of support as recent as Oct 03



Justification

Continued



Need For Space Test

- Correlate behavior of inflatable rigidizable structures in the space environment and on the ground
 - Record deployment characteristics
 - Previous experiments have had unexpected deployment behavior
 - Light-weight and flexibility of materials makes zero-gravity testing essential
 - Determine modal characteristics of deployed tubes to compare with ground test results
 - Modal characteristics crucial for space antennas and other highly sensitive platforms
 - Run a materials analysis on tubes when returned
 - Analyze fiber breakage and delamination of the composite structure

Comparison to Alternatives

- Lower cost, lighter weight, & smaller packaging
- Risk-mitigation experiment for future inflatable/rigidizable missions



History

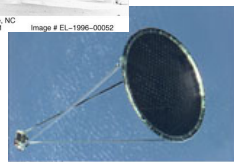


- Some Inflatables in Space
- Some Rigidizables on Earth



Static Inflation Test of 135 Ft Spheroid in Woomersville, NC
NASA Langley Research Center
6/28/1961
Image # EL-1196-00052

ECHO I



IAE



IRSS



IRD

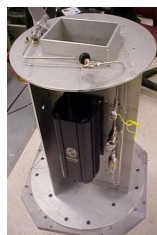
RIGEX will test rigidizable inflatables in the space environment



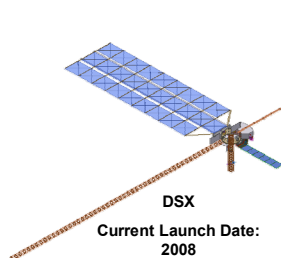
Current / Upcoming Programs



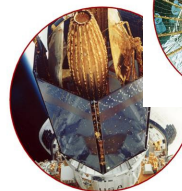
SSP Truss
Ground Testing



RIGEX
Current Launch
Date: 2005



DSX
Current Launch Date:
2008



ISAT
Current Launch
Date: 2015

RIGEX complements ongoing research in inflatable space structures. Various experiments will lead to a Proven Technology:

- SSP Truss – ground testing of various composite material properties
- RIGEX – modal characteristics, deployment, & materials (upon return)
- DSX – radiation effects, lengthy structure deployment, adaptive control
- ISAT – demonstrates load-bearing ability with its instruments



Detailed Overview



Flight / Experiment Data

- 1 self-contained experiment sized for Shuttle CAPE canister, 4 experiment replications
 - No specific orbital requirements
 - No pointing or stabilization requirements
 - No telemetry requirements
 - 1 day mission and return
- Volume: \approx 149000 cc
- Mass: \approx 60kg

Status

- Planned completion of flight article Mar 05

Priority

- 2003 DoD SERB #31
- 2004 AF SERB #17

Requested STP Services

- Launch Services and Integration

Funding

Funding Source	Prior FY (\$k)	FY04 (\$k)	Future FY (\$k)	Total
AFOSR	23.8			23.8
DARPA	20			20
NRO	30			30
AFIT/EN	84.2	15	15	114.2
TOTAL				188k





Summary of Data Application



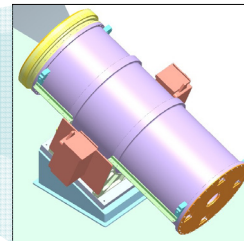
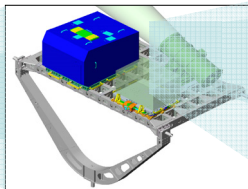
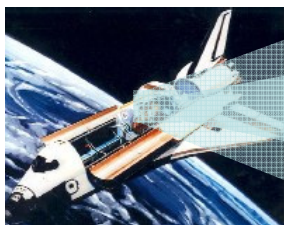
- The Air Force Institute of Technology will use the data from this experiment to validate ground testing methods
- Material data gathered can be applied to all types of inflatable/rigidizable structures & geometries
- Raw and analyzed data will be made available to AFOSR, JPL, DARPA, and NRO as soon as practical
- Applicable category is applied research



RIGEX (AFIT- 0301) FLIGHT MODE SUITABILITY



- | <u>Flight Mode</u> | <u>% Experiment Objectives Satisfied</u> |
|---------------------------------------|--|
| • Shuttle | 100 % |
| • Shuttle Deployable | 0 % |
| • Shuttle Deployable with Propulsion | 0 % |
| • International Space Station | 0 % |
| • "Piggyback" Free-flyer on ELV (GTO) | 0 % |
| • Dedicated Free-flyer on ELV (GTO) | 0 % |
- Value of Flight Hardware Retrieval: Absolutely necessary to retrieve this experiment – all data is collected internally (no telemetry)

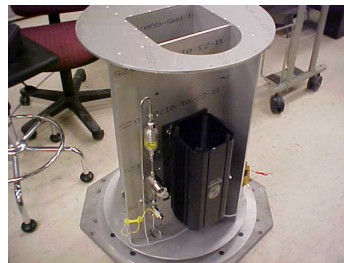
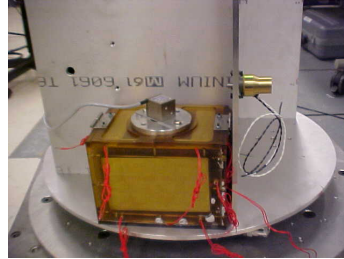




Summary



- The RIGEX CAPE launch is a small-scale, economical payload for STP that will return a great deal of valuable data
- Inflatable/rigidizable structures will have many significant applications in future space systems
- High-potential technology for achieving AF and DoD future needs while lowering launch and life-cycle costs
- The data gained by RIGEX will be a stepping stone to understanding the behavior of inflatable/rigidizables in space and making their use more viable



RIGEX



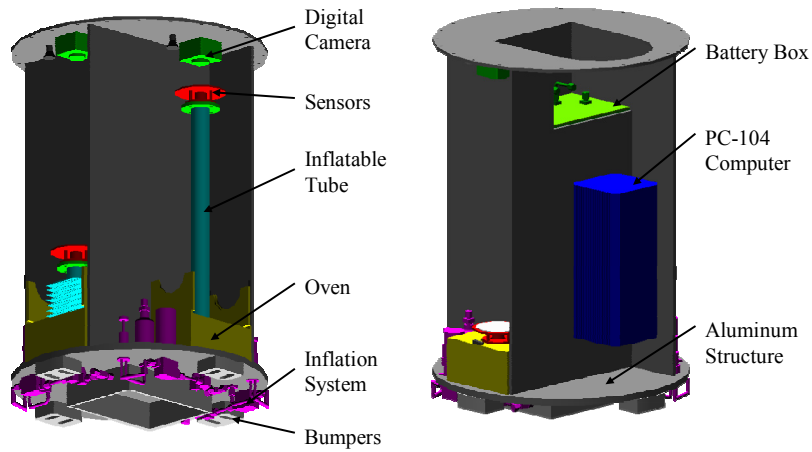
BACKUP SLIDES



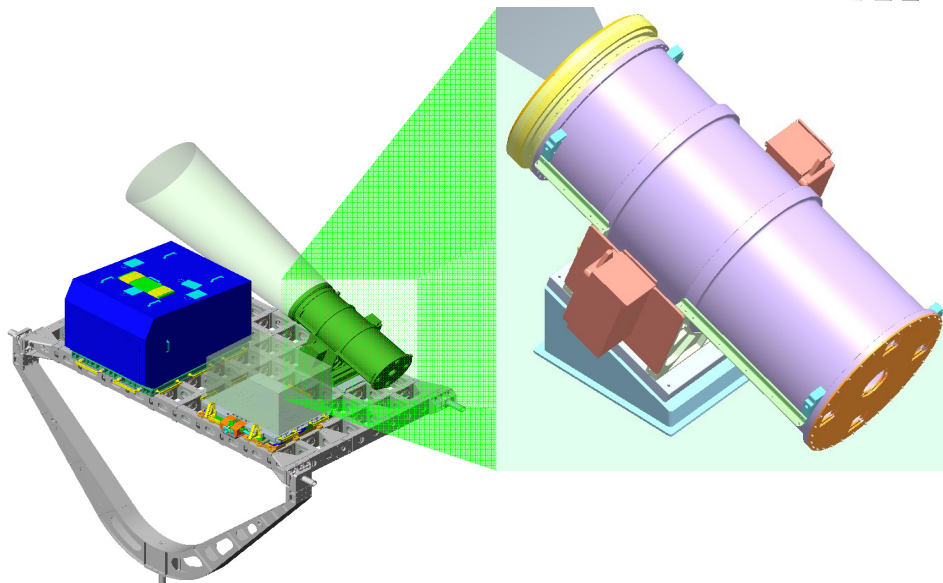
RIGEX System



Detailed Graphic

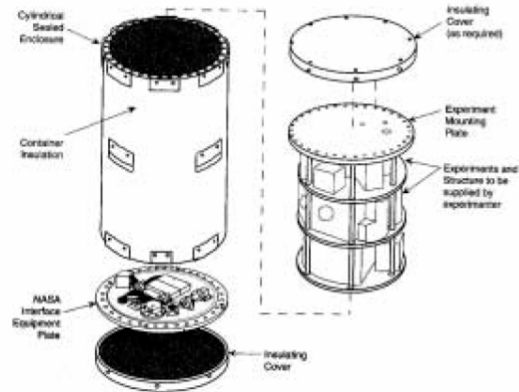


CAPE Configuration





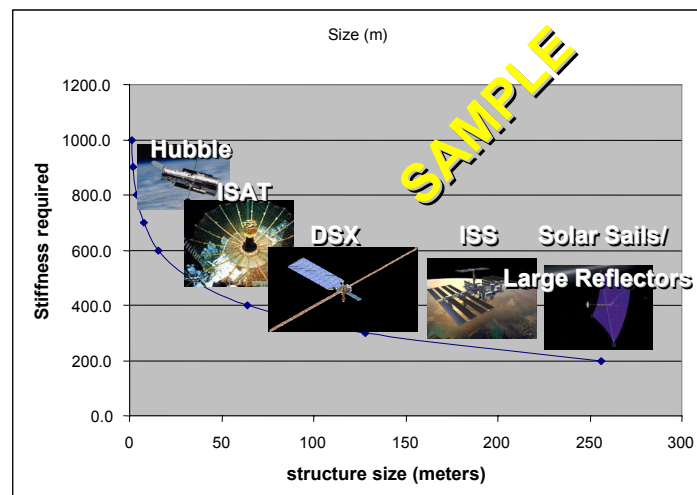
GAS Configuration



Concept Continued

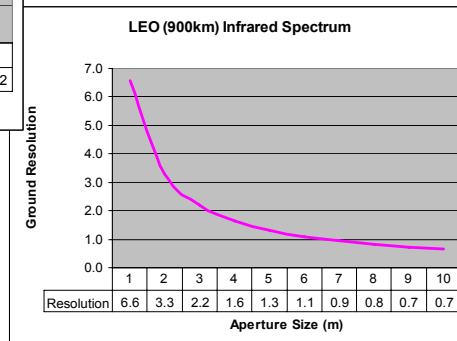
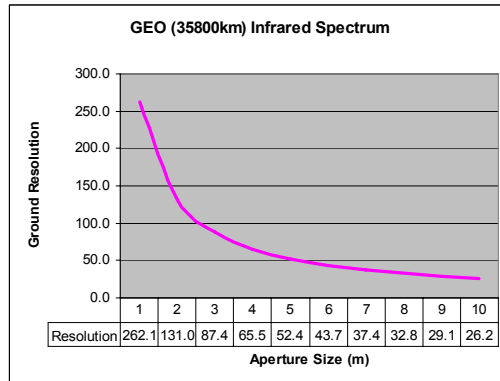


Rigidity Requirements for Various Size Structures





Effects of Aperture Size



NATIONAL RECONNAISSANCE OFFICE
14675 Lee Road
Chantilly, VA 20151-1715



20 October 2003

Major Richard Cobb
Air Force Institute of Technology/ENY
2950 Hobson Way
Wright Patterson AFB, OH 45433

Dear Major Cobb:

I am pleased to provide a letter of support for the Rigidizable Inflatable Get-Away-Special Experiment (RIGEX) program. The National Reconnaissance Office (NRO) has a current and continuing interest in developing various structures for use in space. The use of inflatable rigidized structures for space application is a relatively new area of study with emerging analytical models. However, little or no actual space test data is available.

The Air Force Institute of Technology's RIGEX experiment will provide valuable information on the deployment and modal characteristics of inflatable rigidized tubes. This data can be used by the NRO as a valuable source of risk reduction for future high value missions. RIGEX is a small step towards making inflatables in space a more viable option.

Sincerely,

Alan D. Scott

Alan D. Scott, CAPT, USN
Director, IMINT Research &
Technology Systems Program
Office

Bibliography

1. Ballard, Perry. Chief Engineer, DoD Payloads Office, Johnson Space Center, Houston, Texas. Teleconference. 15 October 2004.
2. Cadogan, David P., Scarborough, Stephen E. *Rigidizable Materials for use in Gossamer Space Inflatable Structures*. AIAA 2001-1417, 42nd Annual AIAA/ASME/ASCE/AHS/ASC Structures, Structural Dynamics, and Materials Conference and Exhibit AIAA Gossamer Spacecraft Forum, Seattle, Washington, 19 April 2001.
3. DiSebastian III, John Daniel. *RIGEX: Preliminary Design of a Rigidized Inflatable Get-Away-Special Experiment*. Master's Thesis, Air Force Institute of Technology, Dayton, OH, March 2001.
4. DoD Shuttle/ISS Payload Support Contract. Muniz Engineering, Inc. *Container for All Payload Ejections (CAPE) Hardware Users Guide (CHUG)*. Houston: Johnson Space Center, 10 March 2003.
5. Freeland, R.E., et al. "Inflatable Deployable Space Structures Technology Summary" American Institute of Aeronautics and Astronautics (IAF-98-1.5.01) (1998).
6. Goddard Projects Directory. <http://library01.gsfc.nasa.gov>. The Goddard Space Flight Center Library, Greenbelt, Maryland. 8 March 2005.
7. Goddard Space Flight Center. *Get Away Special (GAS) Small Self-Contained Payloads—Experimenter Handbook*. NASA, 1995.
8. Guidanean, Koorosh. *An Inflatable Rigidizable Truss Structure Based On New Sub-Tg Polyurethane Composites*. PowerPoint Briefing, L'Garde, Incorporated, Tustin California, 13 October 2004.
9. Holstein III, Raymond G. *Structural Design and Analysis of a Rigidizable Space Shuttle Experiment*. Master's Thesis, Air Force Institute of Technology, Dayton, OH, March 2004.
10. Huang, J., Fang, H., Lovick, R., Lou, M. *The Development of Large Flat Inflatable Antenna for Deep-Space Communications*. AIAA 2004-6112, Space 2004 Conference and Exhibit, San Diego, California, 30 September 2004.
11. Incropera, Frank P., De Witt, David P. *Fundamentals of Heat and Mass Transfer*. 3rd Ed. Canada: John Wiley & Sons, 1990.

12. Kearns, J., et al. *Development of UV-Curable Inflatable Wings for Low-Density Flight Applications*. AIAA 2004-1503, 45th AIAA Gossamer Spacecraft Forum, Palm Springs, California, April 2004.
13. L'Garde Incorporated. <http://www.lgarde.com/index.html>. Homepage. 8 March 2005.
14. Lindemuth, Steven N. *Characterization and Ground Test of an Inflatable Rigidizable Space Experiment*. Master's Thesis, Air Force Institute of Technology, Dayton, OH, March 2004.
15. Lou, M., Fang, H., Hsia, L. *Development of Space Inflatable/Rigidizable STR Aluminum Laminate Booms*. AIAA 2000-5296, Space 2000 Conference and Exposition, Long Beach, California, 21 September 2000.
16. Maddux, Michael. "RIGEX Heater/Storage Box Design and Testing." School of Engineering and Management, Air Force Institute of Technology, Wright-Patterson AFB OH, Summer Quarter 2002.
17. Minco Products, Incorporated. *ThermofoilTM Heaters*. http://www.minco.com/uploadedFiles/Products/Thermofoil_Heaters/Hs202.pdf. Bulletin HS-202(D) Product Catalog. 15 May 2005.
18. Moody, David C. *Microprocessor-Based Systems Control for the Rigidized Inflatable Get-Away Special Experiment*. Master's Thesis, Air Force Institute of Technology, Dayton, OH, March 2004.
19. Omega Engineering, Incorporated. *Product Finder: Thermocouples*. <http://www.omega.com/guides/thermocouples.html>. Omega.com[®]. 15 May 2005.
20. Permatex[®], Incorporated. *Automotive Aftermarket Products Catalog*. http://www.permatex.com/images/catalog/industrial_products/Automotive%20Catalog%20Permatex.pdf. 15 May 2005.
21. Philley, Thomas Lee Jr. *Development, Fabrication, and Ground Test of an Inflatable Structure Space-Flight Experiment*. Master's Thesis, Air Force Institute of Technology, Dayton, OH, March 2003.
22. Ponziani, Kevin. *Image Processing for the Rigidized Inflatable Get-Away-Special Experiment*. Intern Report, Air Force Institute of Technology, Dayton, OH, Unpublished.

23. Satter, C.M., and Robert Freeland. "Inflatable Structures Technology Applications and Requirements." American Institute of Aeronautics and Astronautics (AIAA 95 3737) (1995).
24. Simpson, Andrew, et al. *Flying on Air: UAV Flight Testing with Inflatable Wing Technology*. AIAA 2004-6570, AIAA 3rd "Unmanned Unlimited" Technical Conference, Workshop and Exhibit, Chicago, Illinois, 23 September 2004.
25. Single, Thomas G. *Experimental Vibration Analysis of Inflatable Beams for and AFIT Space Shuttle Experiment*. Master's Thesis, Air Force Institute of Technology, Dayton, OH, February 2002.
26. Smart Material Corporation. *Macro Fiber Composites II*. Data Sheet, Smart Material GmbH, Osprey, Florida, 2003.
27. "Space Test Program Experimenters' Guide." CD-ROM. Produced by the Space Test Program office, Detachment 12, Space and Missile Systems Center, Air Force Space Command. Kirtland Air Force Base, November 2004.
28. Spanjers, Gregory. Project Manager for the Deployed Structures Experiment, Air Force Research Laboratory, Arlington, Virginia, Personal Conversation. 16 November 2004.
29. -----. *Deployed Structures Experiment*, Briefing Presented to the Air Force Space Experiment Review Board, AFRL-0308. 18 August 2004.
30. Steiner M. "Spartan 207 Preliminary Mission Report." Excerpt from unpublished article. n. pag. <http://www.lgarde.com/gsfsc/207.html>. 21 February 1997.
31. Zatman, Michael. Project Manager for Innovative SBR Antenna Technology, DARPA, Arlington, Virginia, Personal Conversation. 16 November 2004.
32. -----. *Innovative SBR Antenna Technology*, Briefing Presented to the DoD Space Experiment Review Board, DARPA-0401. 16 November 2004.

Vita

Capt Chad R. Moeller graduated from Winston Churchill High School in San Antonio, Texas. He entered undergraduate studies at Texas A&M University-Kingsville, Texas where he graduated with a Bachelor of Science Degree in Mechanical Engineering in May 1999. He was commissioned through Air Force Officer Training School in Maxwell, Alabama.

His first assignment was at Travis AFB in May 2000 as a Project Programmer assigned to the 60th Civil Engineering Squadron. While stationed at Travis, he deployed overseas in November 2000 to spend three months at Eskan Village, Kingdom of Saudi Arabia as Chief of the Maintenance Engineering Element. During his final year at Travis, he was reassigned to the Maintenance Engineering Element. In September 2003, he entered the Graduate School of Engineering and Management, Air Force Institute of Technology. Upon graduation, he will be assigned to Cape Canaveral AFS, Florida.

REPORT DOCUMENTATION PAGE				Form Approved OMB No. 074-0188	
<p>The public reporting burden for this collection of information is estimated to average 1 hour per response, including the time for reviewing instructions, searching existing data sources, gathering and maintaining the data needed, and completing and reviewing the collection of information. Send comments regarding this burden estimate or any other aspect of the collection of information, including suggestions for reducing this burden to Department of Defense, Washington Headquarters Services, Directorate for Information Operations and Reports (0704-0188), 1215 Jefferson Davis Highway, Suite 1204, Arlington, VA 22202-4302. Respondents should be aware that notwithstanding any other provision of law, no person shall be subject to a penalty for failing to comply with a collection of information if it does not display a currently valid OMB control number.</p> <p>PLEASE DO NOT RETURN YOUR FORM TO THE ABOVE ADDRESS.</p>					
1. REPORT DATE (DD-MM-YYYY) 13-06-2005		2. REPORT TYPE Master's Thesis		3. DATES COVERED (From – To) June 2004 – June 2005	
4. TITLE AND SUBTITLE Design and Ground-Testing of an Inflatable-Rigidizable Structure Experiment in Preparation for Space Flight				5a. CONTRACT NUMBER	
				5b. GRANT NUMBER	
				5c. PROGRAM ELEMENT NUMBER	
6. AUTHOR(S) Moeller, Chad R., Captain, USAF				5d. PROJECT NUMBER	
				5e. TASK NUMBER	
				5f. WORK UNIT NUMBER	
7. PERFORMING ORGANIZATION NAMES(S) AND ADDRESS(S) Air Force Institute of Technology Graduate School of Engineering and Management (AFIT/EN) 2950 Hobson Way WPAFB OH 45433-7765				8. PERFORMING ORGANIZATION REPORT NUMBER AFIT/GA/ENY/05-J02	
9. SPONSORING/MONITORING AGENCY NAME(S) AND ADDRESS(ES) IMINT/RNTS Attn: Maj. Dave Lee 14675 Lee Road Chantilly VA 20151 DSN: 898-3084 e-mail: David.Lee@nro.mil				10. SPONSOR/MONITOR'S ACRONYM(S)	
				11. SPONSOR/MONITOR'S REPORT NUMBER(S)	
12. DISTRIBUTION/AVAILABILITY STATEMENT APPROVED FOR PUBLIC RELEASE; DISTRIBUTION UNLIMITED.					
13. SUPPLEMENTARY NOTES					
14. ABSTRACT As the demand for larger space structures increases, complications arise including physical dimensions, weight, and launch costs. These constraints have forced the space industry to look for smaller, more lightweight, and cost-effective solutions. Future antennas, solar sails, sun shields, and other structures have the potential to be exponentially larger than their launch envelopes. Current research in this area is focused on the use of inflatable, rigidizable structures to reduce payload size and mass, ultimately reducing launch costs. These structures can be used as booms, trusses, wings, or can be configured to almost any simple shape. More complex shapes can be constructed by joining smaller rigidizable/inflatable members together. Analysis of these structures must be accomplished to validate the technology and gather risk mitigation data before they can be widely used in space applications. The Rigidizable, Inflatable, Get-Away-Special Experiment (RIGEX) was created to test structures that meet the aforementioned demand for smaller, more lightweight, and cost effective solutions to launching payloads into space. The purpose of this experiment is to analyze the effects of the space environment on inflatable, rigidizable structural components and validate ground-test procedures for these structures. This thesis primarily details the pressurization system enhancements and validates thermal performance for RIGEX. These enhancements and the increased knowledge of the thermal properties will improve the probability of experiment success.					
15. SUBJECT TERMS Rigidizable, Inflatable Structures, Space Structure, Space Sciences, Space Technology, Design of Experiments, Experimental Design, CAPE, Sub-Tg					
16. SECURITY CLASSIFICATION OF:			17. LIMITATION OF ABSTRACT UU	18. NUMBER OF PAGES 114	19a. NAME OF RESPONSIBLE PERSON Richard G. Cobb, PhD, AFIT/ENY
a. REPORT U	b. ABSTRACT U	c. THIS PAGE U			19b. TELEPHONE NUMBER (Include area code) (937) 255-3636, ext 4559 (Richard.Cobb@afit.edu)

Standard Form 298 (Rev. 8-98)
Prescribed by ANSI Std. Z39-18